Towards reducing the high cost of parameter sensitivity analysis in hydrologic modelling: a regional parameter sensitivity analysis approach

Samah Larabi[1], Juliane Mai[2], Markus Schnorbus[1], Bryan A. Tolson[2], Francis Zwiers[1]

[1]Pacific Climate Impacts Consortium, University of Victoria, Victoria, British Columbia, Canada

[2]University of Waterloo, Department of Civil and Environmental Engineering, Waterloo, Ontario, Canada

Correspondence to: Samah Larabi (slarabi@uvic.ca)

Abstract. Land surface models have many parameters that have a spatially variable impact on model outputs. In applying these models, sensitivity analysis (SA) is sometimes performed as an initial step to select calibration parameters. As these models are applied on large domains, performing sensitivity analysis across the domain is computationally prohibitive. Here, using a VIC deployment to a large domain as an example, we show that watershed classification based on climatic attributes and vegetation land cover helps to identify the spatial pattern of parameter sensitivity within the domain at a reduced cost. We evaluate the sensitivity of 44 VIC model parameters with regard to streamflow, evapotranspiration and snow water equivalent over 25 basins with a median size of 5078 km^2. Basins are clustered based on their climatic and land cover attributes. Performance of transferring parameter sensitivity between basins of the same cluster is evaluated by the *F1* score. Results show that two donor basins per cluster are sufficient to correctly identify sensitive parameters in a target basin, with *F1* scores ranging between 0.66 (evapotranspiration) to 1 (snow water equivalent). While climatic attributes are sufficient to identify sensitive parameters for streamflow and evapotranspiration, including vegetation class significantly improves skill in identifying sensitive parameters for snow water equivalent. This work reveals that there is opportunity to leverage climate and land cover attributes to greatly increase the efficiency of parameter sensitivity analysis and facilitate more rapid deployment of land surface models over large spatial domains.

1 Introduction

Land surface models (LSMs) are often used over large-scale domains (i.e., continental, or subcontinental river basins) to analyze hydrologic variables of interest. The main purpose of large-domain hydrologic modelling is to simulate, in a spatially consistent manner, the processes governing water fluxes across different geographic and hydroclimatic regions (Mizukami et al., 2017). The application of LSMs over large domains raises several challenges, including the availability of driving data and observations for calibration and the computational cost of calibration.

Parameter estimation when modelling the hydrology of large domains is particularly challenging due the number of parameters that must be estimated, the resulting computational demand and the impact of spatial heterogeneity on parameter transferability. Given the lack of guidance on parameter transferability over large domains, LSMs often rely on a priori parameterizations based on expert opinion, case studies, field data, or hydrologic theory (Beck et al., 2016, Rakovec et al., 2019). Specifically, LSM parametrization of vegetation and soil characteristics is generally based on other measured characteristics or found in the literature from soil and vegetation classes (Nasonava et al., 2009). This approach relies on the assumption that vegetation and soil type solely determine the ideal values of vegetation parameters and soil parameters respectively, neither of which is supported by previous studies (e.g., Rosero et al., 2010; Cuntz et al., 2016; Bennett et al., 2018).

LSM parameter estimation is a high dimensional problem (Göhler et al, 2013; Cuntz et al., 2016). The calibration parameter space can, however, be reduced by a sensitivity analysis (SA) that serves to identify parameters that strongly influence the model output variance. SA provides objective insights on calibration parameters by eliminating parameters from the calibration space that do not affect model output variance (hereafter called noninformative parameters) and reducing the probability of over-parameterization (Van Griensven et al., 2006; Cuntz et al., 2015; Demirel et al., 2018). The computational cost of SA depends on the number of model runs needed to simulate realistic model responses, which increases significantly with the number of model parameters considered (Sarrazin et al., 2016; Devak and Dhanya, 2017). Therefore, SA of LSMs is either overlooked and calibration parameters are selected based on the expert judgement and/or a previous SA, or when performed, the list of model parameters analyzed is artificially shortened to exclude numerous model parameters whose values are not known with certainty. Recent sensitivity analysis studies of LSMs, have however, revealed the impact of fixed-value parameters (i.e., parameters assigned fixed values, often within the model code itself) on model output variance (e.g., Mendoza et al., 2015; Cuntz et al., 2016; Houle et al., 2017), thus raising the need to explore and estimate these parameters to improve the spatial accuracy of LSM outputs and the representation of hydrologic processes.

Sensitivity analysis studies show that parameter sensitivities vary geographically depending on the hydroclimatic conditions (Demaria et al., 2007; Gou et al., 2020) and considered hydrologic processes (Bennett et al., 2018; Sepúlveda et al., 2021). As land surface models are often applied on increasingly larger domains, performing sensitivity analysis across the entire domain to identify the spatial pattern of sensitive parameters becomes increasingly computationally prohibitive, particularly when one considers the large number of parameters involved. In addition, there is a lack of guidance in the literature on ways to extrapolate parameter sensitivity from local to the larger scale with a reduced computational cost.

One approach for extrapolating parameter sensitivity is watershed classification, which aims at identifying watersheds that are similar in some sense (i.e., according to certain attributes). Hydrological applications of watershed classification include understanding general catchment hydrologic behavior (e.g., Sawicz et al., 2011), estimation of flow duration curves and streamflow in ungauged sites (e.g., Boscarello et al., 2016; Kanishka and Eldho, 2020) and estimation of environmental model

parameters in scarce data regions (e.g., Jafarzadegan et al., 2020). In this paper, we investigate the utility of watershed classification for reducing the cost of large-scale parameter sensitivity.

Our objective is to demonstrate the application of watershed classification as a means to regionalize parameter sensitivity. We do this using an example deployment of the Variable Infiltration Capacity model (VIC, Liang et al., 1994, 1996). The VIC model has been extensively used for regional hydrological modelling, but with typically only 4 to 11 parameters adjusted during calibration (e.g., Wenger et al. 2010; Shreshta et al., 2012; Oubeidillah et al., 2013; Schnorbus et al., 2014; Islam et al., 2017; Lohmann et al., 1998; Nijssen et al., 2001; Xie and Yuan, 2006; He and Pang, 2014; Melsen et al., 2016; Yanto et al.,2017; Ismail et al., 2020; Gou et al., 2020; Waheed et al., 2020). Nevertheless, many additional VIC parameters that are typically fixed also affect model output variance (e.g., Mendoza et al., 2015; Melsen et al., 2016; Houle et al., 2017; Bennett et al., 2018). Hence, we examine the regionalization of parameter sensitivity for a much larger suite of 44 parameters that includes 14 soil parameters, four climate parameters, six snow-related parameters, three glacier parameters and 17 vegetation related parameters. In order to address a range of hydrologic processes, parameter sensitivity is assessed with regard to three model outputs: streamflow, evapotranspiration and snow water equivalent.

This paper is organized as follows. Section 2 describes the study area, the VIC-GL model and its parametrization, the sequential screening method and the watershed classification approach used. Section 3 presents the results of the sensitivity analysis for streamflow, evapotranspiration, snow cover, and the results of transferring parameter sensitivity based on watershed classification. Section 4 provides a discussion of the results followed by conclusions in Sect. 5, where we also discuss the implications for cost effective sensitivity analysis when considering hydrologic models with large numbers of parameters that are deployed across large domains.

2 Methods

Section 2.1 presents the study area and the dataset used to drive the VIC-GL model. Section 2.2 describes the version of VIC used here, while Sec. 2.3 describes its parametrization and initialization. The parameter sampling strategy is also described in Sect. 2.3. Section 2.4 presents the Efficient Elementary Effects (EEE; Morris, 1991) screening method used to identify VIC-GL informative parameters. Section 2.5 presents the physical similarity approach used to transfer parameter importance to other basins.

2.1 Study area and dataset

The study area extends over the Pacific Northwest region of North America from 40.75° N to 57.6° N and 109.96° W to 127.9° W (see Fig.1). It encompasses three large watersheds, the Peace, Fraser and Columbia rivers, with a combined area of 1,150,624 km^2. This region spans many physiographic and climatic zones, resulting in substantial hydroclimatic spatial variability. The domain was subdivided into several smaller basins (158 in total) according to location of hydrometric gauges.

91   We selected 25 of these basins representing glacierized conditions in the Coast Mountains and the Rocky Mountains, semi-
92   arid conditions in the interior of both the Fraser and Columbia and in eastern Peace, and the arid conditions of the southern
93   Columbia. The location of these basins is presented in Fig. 1 and their characteristics are summarised in Table 1 and 2. The
94   selected basins capture large spatial variability in precipitation, which is largely controlled by orography, such that average
95   annual precipitation over the 25 basins ranges from 337 mm/year to 1666 mm/year. The sampled basins also capture a strong
96   latitudinal gradient of air temperature, with average annual temperature ranging from -0.37 °C to 7.43 °C. The snow index, the
97   fraction of annual precipitation that falls as snow when temperature is below 2°C (Woods, 2009; Sawicz et al., 2011), ranges
98   from 0.38 to 0.70. The aridity index, the ratio of evapotranspiration to precipitation (ET/P), ranges from 0.28 to 1.66. Average
99   catchment elevation ranges from 683 m to 1990 m.

100
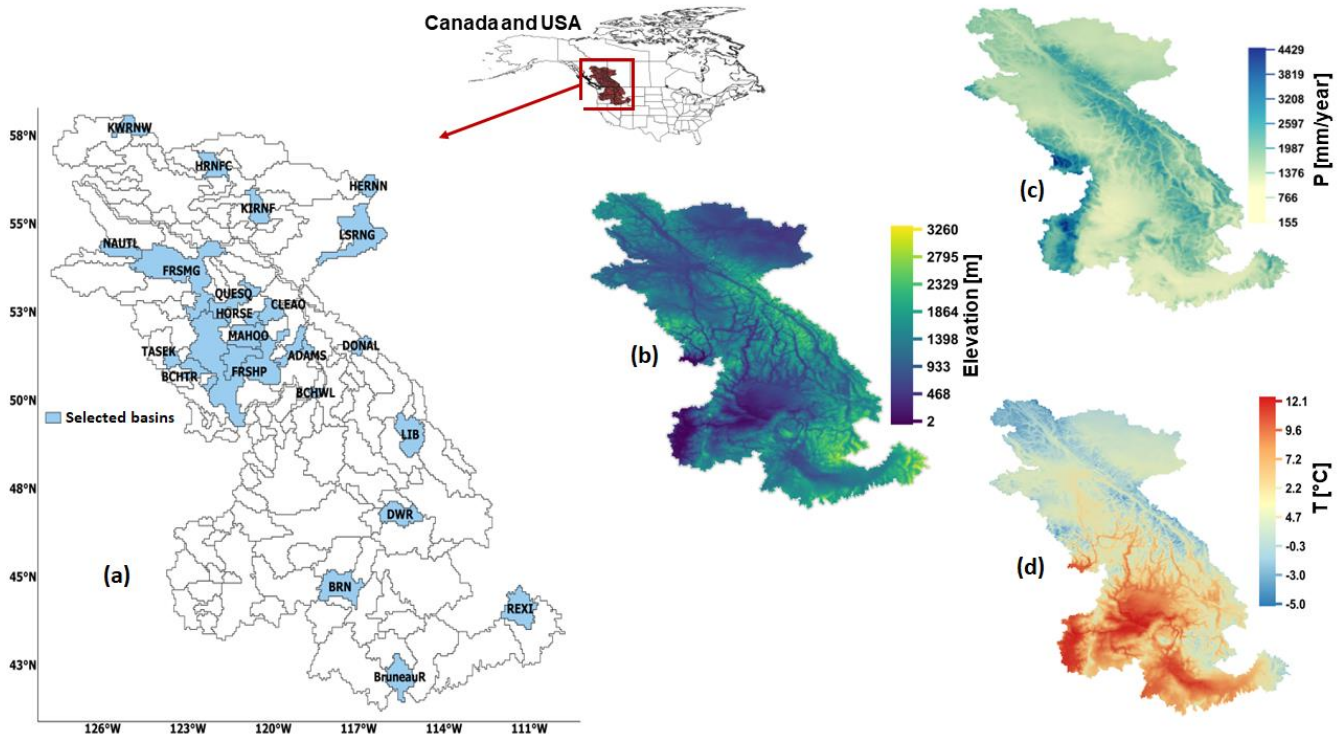
102   **Figure 1: Modelled domain with the location of the 25 selected sub-basins (a), the domain digital elevation map (b), mean annual**
103   **precipitation (c) and mean annual temperature (d), which were calculated from the PNWNAmet dataset.**

104

105

106

 Table 1: Physiographic attributes of 25 selected basins.

Basin ID	Basin name	Basin description	Area [km²]	Glacier area [km²]	Average elevation [m]	Relief [m]
1	ADAMS	Adams River near Squilax, BC	3130	41	1266	1558
2	BCHTR	Bridge River at Terzaghi Dam, BC	2745	54	1748	1434
3	BCHWL	Shuswap River at Wilsey Dam, BC	1021	0	1339	1208
4	BONAP	Bonaparte River below Cache Creek, BC	5334	0	1216	1305
5	BRN	Snake River at Brownlee Dam, Idaho/Oregon	8877	0	1299	1692
6	CAYOO	Cayoosh Creek near Lilooet, BC	954	2	1770	1400
7	CLEAO	Clearwater River at the outlet of Clearwater Lake, BC	3031	224	1625	1540
8	DONAL	Columbia River at Donald, BC	1623	115	1767	1838
9	DWR	North Fork Clearwater River at Dworshak Dam, ID	6066	0	1307	1341
10	FRSHP	Fraser River at Hope, BC	31557	62	1198	2015
11	FRSMG	Fraser near Marguerite, BC	20810	0	867	968
12	HERNN	Krawchuk Drainage near Mclennan, BC	4018	0	683	160
13	HORSE	Horsefly River above McKinley Creek, BC	1242	0	1400	990
14	KIRNF	Kiskatinaw River near Farmington, BC	6196	0	910	555
15	LIB	Kootenai River at Libby Dam, MT	6977	0	1327	1240
16	LSRNG	Little Smoky River near Guy, AB	18975	0	868	946
17	MAHOO	Maood River at outlet of Mahood Lake, BC	5078	0	1194	1072
18	NAUTL	Nautley river near Fort Fraser, BC	3163	0	956	565
19	QUESQ	Quesnel River near Quesnel, BC	5551	78	1251	1442
20	SEYMO	Seymour River near Seymor Arm, BC	1024	41	1516	1422
21	TASEK	Taseko River at outlet of Taseko Lake, BC	1789	194	1990	1098
22	REXI	Henrys Fork Rexburg, ID	8034	0	1983	1590
23	BurneauR	Bruneau River near Hot Spring, Idaho	7074	0	1711	1852
24	KWRNW	Kwadacha River Near Ware, BC	5034	144	1538	1433
25	HRNFC	Halfway River near Farrel Creek, BC	5906	0	835	705

110 The climatic attributes presented in Table 2 are spatially averaged by sub-basin from the gridded PNWNAmet dataset (Werner
111 et al., 2019), which is used to drive the VIC model. This dataset provides gridded observations of daily precipitation (mm) and
112 minimum and maximum temperature (°C) for the Northwestern North America. The dataset is available at a daily timestep
113 and a spatial resolution of 1/16° for the period 1945 to 2012. Wind speed (m/s) from the 20CR reanalysis (Compo et al., 2011)
114 that has been spatially interpolated to 1/16° is also provided with the PNWNAmet dataset at a daily timescale. For further
115 details see Werner et al. (2019).

116 **Table 2: Climatic attributes of the 25 selected basins.**

Basin name	Average annual precipitation [mm]	Average annual temperature [°C]	Snow index	Aridity index
ADAMS	1196	3.39	0.47	0.40
BCHTR	1123	1.42	0.62	0.37
BCHWL	991	3.64	0.51	0.48
BONAP	475	3.88	0.43	1.04
BRN	557	7.42	0.40	1.01
CAYOO	995	1.93	0.60	0.43
CLEAO	1492	1.00	0.57	0.28
DONAL	1194	0.23	0.61	0.34
DWR	1271	5.88	0.48	0.41
FRSHP	951	3.96	0.44	0.51
FRSMG	634	2.94	0.44	0.76
HERNN	448	1.23	0.47	1.14
HORSE	1119	2.17	0.51	0.40
KIRNF	575	2.19	0.45	0.87
LIB	856	3.93	0.48	0.56
LSRNG	570	2.62	0.41	0.90
MAHOO	675	3.34	0.45	0.72
NAUTL	583	2.64	0.45	0.82
QUESQ	939	2.86	0.46	0.50
SEYMO	1666	2.63	0.70	0.28
TASEK	1310	-0.37	0.70	0.29
REXI	729	3.54	0.54	0.65
BruneauR	337	7.43	0.38	1.66
KWRNW	845	-1.57	0.62	0.47
HRNFC	514	1.61	0.48	0.96

2.2 VIC-GL model

VIC is a physically based macroscale model that simulates both water and energy balances by grid cells (Liang et al., 1994, 1996; Cherkauer and Lettenmaier, 1999). The VIC model has been widely applied to analyze the impact of climate change on the hydrology and water resources of the study region (e.g., Hamlet and Lettenmaier, 1999; Payne et al., 2004; Shrestha et al., 2012; Schnorbus et al., 2014; Islam et al., 2017) and to study the effect of land cover change on streamflow (e.g., Matheussen et al., 2000). VIC-GL, an upgraded version developed at the Pacific Climate Impacts Consortium (PCIC) that is used here, includes additional functionality to simulate glacier mass balance (Schnorbus, 2018). VIC-GL was branched from VIC version 4.2, and although the model physics are in many ways similar, it uses a different model abstraction from its predecessor. Although the computational domain of VIC-GL is still described using a two-dimensional grid (using a spatial resolution of 1/16° in the current application), sub-grid variability in land cover and topography uses hydrologic response units (HRUs) as opposed to the original vegetation tiles. Specifically, an HRU is assigned for each land cover class within an elevation band, with the elevation of each HRU being the median of the associated elevation band. In this manner, the type and extent of land cover is allowed to vary with elevation within grid boxes. The vertical water and energy balance is solved separately in each HRU and then averaged to the grid-cell scale. The current application of VIC-GL uses fixed 200-m elevation bands and three soil layers. The baseline model processes are described in detail by Liang et al. (1994, 1996), Cherkauer et al. (2013) and Bohn et al. (2016).

Updates to address glacier mass balance modelling are described in detail by Schnorbus (2018), but pertinent VIC-GL parameter changes are summarised here. Glacier surface mass and energy balance modelling introduces three additional parameters *GLAC_ALB*, *GLAC_ROUGH* and *GLAC_REDF*. *GLAC_ALB* specifies the albedo of glacier ice, which controls the amount of incoming solar radiation absorbed by the ice surface. The value of *GLAC_ALB*, once set, is constant in time. The parameter *GLAC_ROUGH* specifies the roughness length of the glacier surface, which affects the wind speed profile and the transfer of energy to the glacier surface due to the turbulent fluxes. The scaling factor for snow redistribution (*GLAC_REDF*) controls the redistribution of precipitation between non-glacier HRUs and acts as a proxy for mechanical snow redistribution that typically occurs via wind and gravity in mountainous alpine environments (e.g. Kuhn 2003). VIC-GL also uses the rain-snow partitioning algorithm of Kienzle (2008) rather than the original algorithm in the VIC model distribution. This is a curvilinear model that uses two parameters, the threshold mean daily temperature (*TEMP_TH_1*), where 50% of precipitation falls as snow, and the temperature range centered on *TEMP_TH_1* within which both solid and liquid precipitation occurs (*TEMP_TH_2*). VIC-GL has also been updated to make certain parameters more accessible for model calibration and to allow for a more spatially explicit description of some hydro-climatic processes. These parameters include five that determine soil albedo decay according to the USACE algorithm (USACE 1956) and the climatic parameters *T_LAPSE* and *PGRAD*. The latter specify vertical temperature and the precipitation gradients that are used to adjust temperature and precipitation, respectively, for each HRU within a grid cell.

2.3 Model parameterization and sampling

150 We consider 44 VIC-GL parameters (Table 3) composed of 5 baseflow parameters, 1 runoff parameter, 9 drainage parameters,

151 4 climate parameters, 6 snow-related parameters, 3 glacier parameters and 17 vegetation related parameters. The set of

152 analyzed parameters includes the commonly calibrated parameters, parameters that have been addressed in previous studies

153 (e.g., Demaria et al., 2007; Houle et al., 2017; Bennett et al., 2018), and some that are typically set to fixed values (Gao et al.,

154 2009).

155

156 **Table 3: The 44 VIC-GL parameters selected for the sensitivity analysis.**

Parameter	Description	Unit	Range	Default	Type*
Baseflow parameters					
ds	Fraction of Dsmax where nonlinear baseflow begins	_	[0.001, 0.6]	0.1	Absolute
dsmax	Maximum velocity of baseflow	mm/day	[1, 200]	40	Absolute
ws	Fraction of maximum soil moisture where nonlinear baseflow occurs	_	[0.4, 1]	0.9	Absolute
c	Exponent used in baseflow curve	_	[1, 10]	2	Absolute
depth3	Thickness of soil layer 3	m	[0.5, 10]	2	Absolute
Runoff parameters					
INFIL	Variable infiltration curve parameter	_	[0.0001, 0.8]	0.2	Absolute
Drainage parameters					
watn	Exponent in Campbell's equation for hydraulic conductivity in all layers	_	[8, 11]	9.5	Absolute
ks	Saturated hydrologic conductivity in all layers	mm/day	[300, 3000]	1081	Absolute
depth1	Thickness of soil layer 1	m	[0.001, 0.5]	0.1	Absolute
depth2	Thickness of soil layer 2	m	[0.05, 1]	0.2	Absolute
bd	Soil bulk density (applied to all layers)	kg/m^3	[800, 1600]	1400	Absolute
sdens	Soil particle density (applied to all layers)	kg/m^3	[2000, 2700]	2500	Absolute
wcr	Critical Point (applied to all layers)	_	[0.35, 0.55]	0.40	Absolute
wpwp	Wilting point (applied to all layers)	_	[0.20, 0.50]	0.35	Absolute
resid_moist	Residual moisture (applied to all layers)	_	[0.0, 0.125]	0.08	Absolute
Climate parameters					
PGRAD	Precipitation gradient	1/m	[0.0001, 0.001]	0.0005	Absolute
T_LAPSE	Temperature lapse rate	°C/m	[0, 9.5]	6.5	Absolute

TEMP_TH_1	Rain/snow temperature threshold parameter 1	°C	[-2.0, 5.0]	2	Absolute
TEMP_TH_2	Rain/snow temperature threshold parameter 2	°C	[8.0, 15.0]	12	Absolute
Snow parameters					
SNOWROUGH	Surface roughness of snowpack	m	[0.0001, 0.1]	0.01	Absolute
NEW_SNOW_ALB	Albedo of new snow	_	[0.8, 0.9]	0.85	Absolute
SNOW_ALB_ACCUM_A	Albedo decay coefficient during accumulation period	_	[0.3, 0.99]	0.94	Absolute
SNOW_ALB_ACCUM_B	Albedo decay exponent during accumulation period	_	[0, 0.99]	0.58	Absolute
SNOW_ALB_THAW_A	Albedo decay coefficient during thaw period	_	[0.1, 0.99]	0.82	Absolute
SNOW_ALB_THAW_B	Albedo decay exponent during thaw period	_	[0, 0.99]	0.46	Absolute
Glacier parameters					
GLAC_ALB	Albedo of glacier surface	_	[0.2, 0.6]	0.4	Absolute
GLAC_ROUGH	Surface roughness of glacier	m	[0.0001, 0.01]	0.001	Absolute
GLAC_REDF	Scaling factor for snow redistribution with values in range 0 (no redistribution) to 1 (redistribution equal to area ratio)	_	[0, 1]	0	Absolute
Vegetation parameters					
root_depth	Thickness of root zone layer 3	m	[0.5, 2]	1	Multiplicative factor
root_fract1	Fraction of roots in soil layer 1	_	[0, 1]	0.7	Absolute
root_fract2	Fraction of roots in soil layer 2	_	[0, 1]	0.2	Absolute
lai_djf	Leaf Area Index (winter)	m2/m2	[0.5, 2]	1	Multiplicative factor
lai_mam	Leaf Area Index (spring)	m2/m2	[0.5, 2]	1	Multiplicative factor
lai_jja	Leaf Area Index (summer)	m2/m2	[0.5, 2]	1	Multiplicative factor
lai_son	Leaf Area Index (fall)	m2/m2	[0.5, 2]	1	Multiplicative factor
alb_dja	albedo(winter)	_	[0.5, 2]	1	Multiplicative factor
alb_mam	albedo(spring)	_	[0.5, 2]	1	Multiplicative factor
alb_jja	albedo(summer)	_	[0.5, 2]	1	Multiplicative factor
alb_son	albedo(fall)	_	[0.5, 2]	1	Multiplicative factor
Rarc	Architectural resistance	s/m	[0.5, 2]	1	Multiplicative factor
Rmin	Minimum stomatal resistance	s/m	[0.5, 2]	1	Multiplicative factor

RGL	Minimum incoming shortwave radiation at which there will be transpiration	W/m^2	[0.5, 2]	1	Multiplicative factor
SolAtn	Solar attenuation factor	_	[0.5, 2]	1	Multiplicative factor
WndAtn	Wind speed attenuation through the overstory	_	[0.5, 2]	1	Multiplicative factor
Trunk_ratio*	Ratio of total tree height that is trunk	_	[-0.2, 0.2]	0	Additive change

157 *Type is the parameter sampling strategy, which is to either replace the parameter default value (i.e., Absolute), apply a
158 multiplicative factor or apply an additive change to the baseline values. The additive change is applied so that trunk ratio
159 remains between 0.1 and 0.8.

160 The commonly calibrated parameters are limited to four baseflow parameters, the runoff parameter, and five drainage
161 parameters. The common baseflow parameters are maximum velocity of baseflow (*dsmax),* fraction of *dsmax* where nonlinear
162 baseflow begins *(ds)*, fraction of maximum soil moisture where non-linear baseflow occurs *(ws)* and thickness of deepest soil
163 layer *(depth3).* These parameters describe the non-linear relationship between baseflow rate and soil moisture in the deepest
164 soil layer (with thickness described by *depth3*). The runoff parameter, or variable infiltration curve parameter *(INFIL),*
165 describes the extent of soil saturation within grid cell (i.e., amount of direct runoff) as function of soil moisture in the surface
166 soil layers (i.e., the variable infiltration curve, Liang et al., 1994) which have thicknesses given by *depth1* and *depth2*. The
167 common drainage parameters are the two parameters controlling soil storage capacity (*depth1* and *depth2*), the exponent in
168 Campbell's equation for hydraulic conductivity (*watn*) and the saturated hydrologic conductivity (*ks*).

169 The additional drainage parameters considered are the soil bulk density (*bd*), soil particle density (*sdens*), fractional soil
170 moisture content at the critical point (*wcr*), fractional soil moisture content at the wilting point (*wpwp*) and the residual moisture
171 (*resid_moist*). The *wpwp* parameter dictates baseflow estimation with the ARNO model formulation (Francini and Pacciani,
172 1991) used in VIC (Gao et al., 2009). We also consider the four climate parameters which are temperature lapse rate
173 (*T_LAPSE*), precipitation gradient, and the rain/snow temperature threshold parameter 1 and 2 (*TEMP_TH_1 and*
174 *TEMP_TH_2).* The examined parameters also include the three glacier mass balance parameters (*GLAC_ALB, GLAC_ROUGH*
175 *and GLAC_REDF*). The snow related parameters examined are surface roughness (*SNOWROUGH*), albedo of new snow
176 (*NEW_SNOW_ALB*) and albedo decay parameters during the accumulation period (*SNOW_ALB_ACCUM_A,*
177 *SNOW_ALB_ACCUM_B*) and during the thaw period (*SNOW_ALB_THAW_A, SNOW_ALB_THAW_B*).

178 The parameters describing snow and glacier properties along with soil and climate parameters are assigned by grid cell. These
179 parameters were initialized with default values and then sampled within prescribed ranges (see Table 3).The same value is
180 assigned to all grid cells within a catchment. The sampling of the soil parameters critical point (*wcr*), wilting point (*wpwp*) and
181 residual moisture (*resid_moist*) is constrained so that conditions required by VIC (Gao et al., 2009) are not violated. Thus,
182 sampling is performed so that $wcr \leq (1 - bd/sdens)$, $wpwp \leq wcr$, and $resid\_moist \leq wpwp * (1 - bd/sdens)$.

183 The vegetation parameters consist of the thickness of root zone of the third soil layer (*root_depth*), and the root fractions in all

184 three soil layers. We only sample root fractions in soil layer one and two (*root_fract1*, *root_fract2)* such that the total root

185 fraction in the three soil layers adds to 1. That is, the *root fraction* in soil layer three is updated as 1 - (*root_fract1 + root_fract2*).

186 The vegetation parameters that are considered also include the seasonal leaf area index (*lai*) and seasonal albedo (*albedo*), the

187 architectural resistance (*Rarc*), minimum stomatal resistance (*Rmin*), minimum incoming shortwave radiation at which there

188 will be transpiration (*RGL*), solar attenuation factor (*SolAtn*), wind speed attenuation through the overstory (*WndAtn*) and

189 fraction of the total tree height that is occupied by tree trunks (*Trunk_ratio*). The *lai* parameter governs the amount of water

190 intercepted by the canopy, which controls canopy evaporation. Leaf area index, along with stomatal resistance (*Rmin*), also

191 influences the estimation of vegetation transpiration, and the root fraction dictates the amount of transpiration from each soil

192 layer (Gao et al., 2009). The parameter *Rarc* affects the vertical wind profile.

193 The vegetation parameters are assigned by land cover class. Sampling of these parameters is conducted by adjusting baseline

194 values obtained for each land cover class. The land cover classes were based on the North America Land Cover dataset,

195 edition2 (Natural Resources Canada/The Canada Centre for Mapping and Earth Observation (NRCan/CCMEO) et al. 2013)

196 produced as part of the North America Land Change Monitoring System (NALCMS). In total, 22 land cover classes were

197 identified. For most of these parameters, sampling is conducted by applying a multiplication factor, sampled in the range 0.5

198 to 2.0, to the baseline values. The same sampled parameter is applied to all vegetation classes. To reduce the number of

199 vegetation parameters, a multiplier factor is applied on a seasonal basis for the monthly parameters *LAI* and *albedo*, following

200 a similar approach of Bennett et al., (2018). For example, *lai_djf* is the multiplier factor applied to leaf area index values during

201 winter months (i.e., December, January, and February). The *trunk ratio* is sampled around the defined value by applying an

202 additive change in the range -0.2 to 0.2 so that *trunk ratio* values remain between 0.1 and 0.8. The monthly roughness and

203 displacement height parameters were not sampled. They are specified as a function of vegetation height (which is constant

204 within classes, but variable between classes) and leaf area index as described by Choudhury and Monteith (1988).

2.4 Sensitivity analysis

206 We applied the Efficient Elementary Effects (EEE) screening method introduced by Cuntz et al. (2015) as a frugal

207 implementation of the Morris method (Morris, 1991). It was developed to identify the model parameters that are most

208 informative regarding a certain model output. The strength of the method lies in it requiring only a small set of model

209 evaluations to separate informative vs. noninformative parameters. On average, EEE requires 10N model runs with N being

210 the number of model parameters. EEE does not require algorithmic tuning and converges by itself. The method has been tested

211 for a large range of sensitivity benchmarking functions and a hydrologic model at several locations by Cuntz et al. (2015). The

212 method has further been applied to obtain the informative parameters in complex hydrologic (Cuntz et al., 2016) and land-

213 surface models (Demirel et al., 2018).

214   The EEE approach samples model parameters in trajectories as initially described by Morris (1991) and improved by

215   Campolongo et al. (2007). A "trajectory" is defined as a sequence of ($N+1$) parameter sets where the first parameter set is

216   sampled randomly while all subsequent sets i ($i > 1$) differ from the prior set (i-1) in exactly one parameter value. Such

217   trajectories allow an efficient sampling of the whole parameter space while considering parameter interactions to a certain

218   extent. In the approach of Cuntz et al. (2015), only a small number of such trajectories (M_1; here M_1=5) are sampled in a first

219   EEE iteration to lower the computational burden. The resulting ($M_1 \times (N + 1)$) model outputs are derived, and the elementary

220   effects (EEs) are computed for each parameter following Morris (1991). The elementary effect (EE) quantifies the change in

221   model output $f(p)$ when a parameter p_i is changed by a fraction of this parameter range Δ. The elementary effect of parameter

222   p_i is calculated as follows:

223    $EE_i = \frac{f(p_i+\Delta)-f(p_i)}{\Delta}$ (1)

224   The EEs are used to identify the most informative parameters by deriving a threshold that splits the parameters into a set of

225   N_{ninf} noninformative parameters and a set of $N_{inf}=N-N_{ninif}$ informative parameters. The threshold T is derived automatically

226   within the EEE method and is based on the EEs of the model outputs provided in the first iteration. The threshold is derived

227   based on fitting a logistic function to the sorted EEs derived and defining the threshold as the point of largest curvature of the

228   fitted logistic function. Defining the threshold that is used to separate informative and non-informative parameters in this

229   approach has been demonstrated using a wide range of test functions and real-world examples, and the reader is referred to

230   Cuntz et al. (2015) for further details. In the next EEE iteration, a new N-dimensional parameter set is randomly sampled but

231   this time only the N_{ninf} noninformative parameters are perturbed while the N_{inf} informative parameters are kept at their initially

232   sampled values. Hence, this trajectory contains only N_{ninf}+1 parameter sets. M_2 of such trajectories are sampled in this step

233   (here M_2=1). The derivation of model outputs and the calculation of EEs is repeated. If the EE of any noninformative parameter

234   exceeds the previously derived threshold T, the previously noninformative parameter will be added to the set of informative

235   parameters. This EEE iteration (sampling a new trajectory and then adding parameters with an EE above T to the set of

236   informative parameters) is repeated until no further parameter is reclassified as informative. The final EEE iteration is to

237   sample M_3 trajectories (here M_3=5) to confirm that the set of N_{ninf} noninformative parameters is stable, and no further parameter

238   is found to be informative. The EEE method parameter values (M_1, M_2, and M_3) utilized here are the default settings tested and

239   recommended by Cuntz et al. (2015). The implementation, documentation, and examples for EEE are open source (Mai and

240   Cuntz, 2020).

241   **2.5 Transferability of parameter sensitivity**

242   We applied the EEE method to each of the 25 basins and the three model outputs (streamflow, evaporation, snow water

243   equivalent) independently, leading to 75 sets of noninformative/informative parameters. The initial set of N randomly sampled

244   model parameter values was the same for all 75 experiments. An average of 430 model runs were required for all 75 EEE

245   experiments to identify which of the 44 VIC-GL parameters analyzed in this study were informative.

246 Informative and noninformative parameters were compared over the 25 basins to identify parameters that are informative
247 across all basins (termed invariant-informative parameters), 2) parameters that are non-informative across all basins (invariant-
248 noninformative, and 3) parameters that are informative in some basins but not others (variant-informative).

249 We evaluated the potential of using watershed classification as a tool to transfer parameter SA information. Climatic conditions
250 exert a major control on runoff generation (Yadav et al., 2007; Sawicz et al., 2011) and have been found to have a higher
251 impact on parameter sensitivity than vegetation and soil conditions (Rosero et al., 2010). However, vegetation and soil
252 conditions can affect other hydrologic quantities. For example, Bennett et al. (2018) found that canopy spacing plays an
253 important role in snow water equivalent simulation by VIC. Here, we used aridity index, snow index and the percentage of
254 glacier area, and the percentage of area covered by each of several vegetation classes to classify the 25 basins. Although 22
255 vegetation classes are defined for VIC-GL, we only considered the four vegetation classes listed in Table 4 that are dominant
256 in the study area. To evaluate the impact of vegetation on informative parameter identification, watershed classification was
257 first performed using the climatic attributes only, and then by combining climatic and vegetation class cover attributes.
258
259 **Table 4: Statistics of the percentage of VIC land cover classes (%) identified using NALCMS and considered in this study over the**
260 **25 selected basins.**

Class ID	Description	Min	Max	Mean
2	Temperate or sub-polar needleleaf forest - high-elevation	0.1	46	18
4	Temperate or sub-polar needleleaf forest - coastal/humid/dense	0	29	9
9	Mixed Forest	0	34	4
11	Temperate or sub-polar shrubland	0.4	91	19

261 To classify the 25 basins into homogenous groups, the agglomerative hierarchical algorithm was used with the Euclidean
262 distance and Ward's criterion (Roux, 2018). Agglomerative hierarchical clustering consists of a series of successive fusion of
263 watersheds into groups according to their similarity. It starts by considering each element x (i.e., watershed) as a cluster {x}
264 then continue by creating new cluster by merging the two closest clusters. The dendogram, a tree diagram, illustrates the
265 merging process of the agglomerative hierarchical clustering. The Ward method used here aggregates clusters so that within-
266 group inertia (i.e. multidimensional variance) is minimal.

267 To test our hypothesis that parameter sensitivity can be generalized using watershed classification we conducted the following
268 evaluation. Each sub-basin was set as the target basin. For each target basin, informative parameters are transferred using a
269 number of donor basins of the same cluster. Using multiple donor basins has been shown to provide better results than a single
270 donor basin (e.g. Oudin et al., 2008; Bao et al., 2012). Let A be a target basin of cluster C_i. We assume that informative
271 parameters of basin A are the intersection of informative parameters of x donor basins from cluster C_i. For each target basin

272 A, informative parameters are transferred using all possible combinations of x donor basins of cluster C_i not including A. This

273 test aims at evaluating whether x donor basins could be used to generalize informative parameters for each cluster.

274 The performance of watershed classification to identify informative and noninformative parameters in a basin is evaluated

275 using the *F1* score. This score is often used to measure the performance of a binary classification (Chicco and Jurman, 2020).

276 The *F1* score is a weighted average of precision and recall. Assuming two classes, positive (informative) and negative

277 (noninformative), the *F1* score measures the ability to correctly and incorrectly predict the two classes. Considering counts of

278 TP true positive (i.e., informative predicted as informative), FP false positive (informative predicted as noninformative), and

279 FN false negative (noninformative predicted as informative), we can obtain measures of precision, recall and the *F1* score as

280 follows:

281 $Precision = \frac{TP}{TP+FP}$, (2)

282 $Recall = \frac{TP}{TP+FN}$, (3)

283 $F1\ score = 2 * \frac{Precision \times Recall}{Precision + Recall}$ (4)

284

285 The *F1* score takes values between 0 and 1, where 0 means that all positive (here informative parameters) are predicted as

286 negative (i.e., as noninformative) and 1 means perfect classification with *FN=FP=0*.

287 For a given number of donor basins x, the *F1* score is reported for each target basin A as the average *F1* score calculated

288 between sensitive parameters of A and identified sensitive parameters from all possible combinations of the x donor basins.

289 This is done for each classification method, climate-based and climate-land cover-based clustering, to evaluate performance

290 in identifying sensitive parameters by watershed groupings provided by each clustering analysis. Then, we use the Wilcoxon

291 signed rank test to compare the *F1* scores for the 25 basins obtained using the two clustering methods so that we can determine

292 whether incorporating land cover in watershed classification improves the ability to predict informative parameters. The

293 Wilcoxon signed rank test tests the null hypothesis that the *F1* score resulting from both clustering analyses are from the same

294 distribution i.e., have similar ability to identify informative parameters.

295 **3 Results**

296 The sensitivity analysis using the EEE method was performed with respect to three model outputs independently: streamflow,

297 evapotranspiration, and snow water equivalent. Figure 2 presents the number of occurrences of informative parameters over

298 the 25 selected sub-basins for the three outputs. From this figure, we can identify the three parameter categories, invariant-

299 informative, invariant noninformative and variant-informative for each hydrologic process. Table 5 summarizes the three

300 parameter categories per model output. Amongst the 44 VIC-GL parameters only 9 parameters are invariant-informative for

301 streamflow, 13 are invariant-informative for evapotranspiration and 4 are invariant-informative for snow water equivalent. A

302 large percentage of parameters are variant-informative for these fluxes with 29 parameters for streamflow, 25 parameters for

303 evapotranspiration and 14 parameters for snow water equivalent. We first examine the sensitive parameters and their spatial

304 variability per model output in Sect. 3.1 to 3.3. We further analyze the performance of the physical similarity approach for

305 transferring sensitivity analysis information and the attributes that are informative for each model output (Sect. 3.4).

306
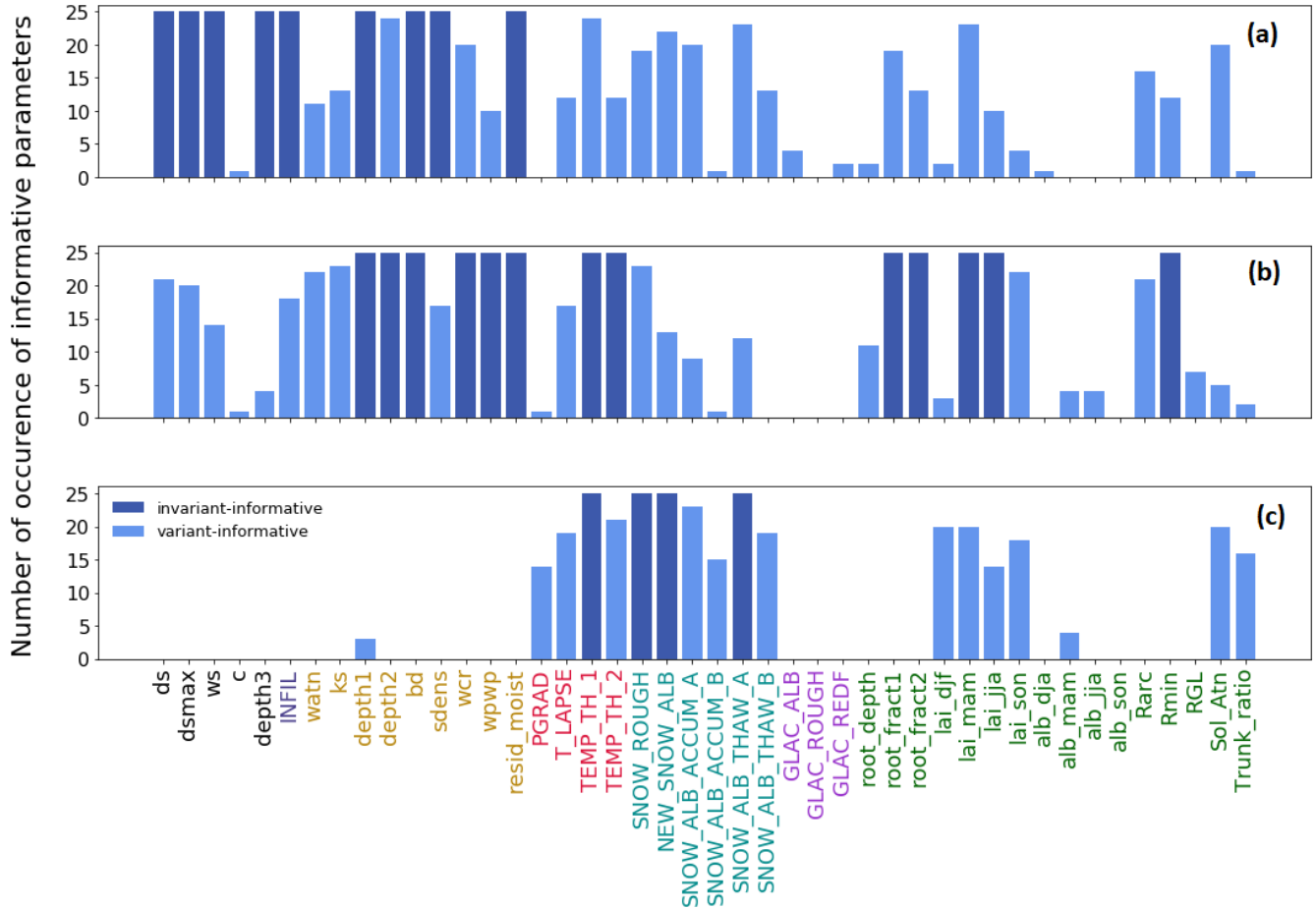
307
308 **Figure 2: Number of occurrences of informative parameters for streamflow (a), evapotranspiration (b) and snow water equivalent**
309 **(c) over the 25 studied sub-basins. Parameters are considered invariant-informative if the count of basins in which they are**
310 **informative equals 25, invariant-noninformative if that count is 0, and variant-informative if the count is between 1 and 24.**

311

Table 5: VIC-GL parameter importance regarding streamflow, evapotranspiration (ET) and snow water equivalent (SWE).

Process	Invariant-informative parameters	Invariant-noninformative parameters	Variant-informative parameters
Streamflow	ds, dsmax, ws, depth3, INFIL, depth1, bd, sdens, resid_moist	PGRAD, GLAC_ROUGH, alb_mam, alb_jja, alb_son, RGL	c, T_LAPSE, watn, ks, depth2, wcr, wpwp, SNOW_ROUGH, NEW_SNOW_ALB, SNOW_ALB_ACCUM_A, SNOW_ALB_ACCUM_B, SNOW_ALB_THAW_A, SNOW_ALB_THAW_B, TEMP_TH_1, TEMP_TH_2, GLAC_ALB, GLAC_REDF, root_depth, root_fract1, root_fract2, lai_djf, lai_mam, lai_jja, lai_son, alb_dja, Rarc, Rmin, Sol_Atn, Trunk_ratio
ET	depth1, depth2, bd, wcr, wpwp, resid_moist, TEMP_TH1, TEMP_TH2, root_fract1, root_fract2, lai_mam, lai_jja, Rmin	SNOW_ALB_THAW_B, GLAC_ALB, GLAC_ROUGH, GLAC_REDF, alb_dja, alb_son	ds, dsmax, ws, c, depth3, INFIL, PGRAD, T_LAPSE, watn, ks, sdens, SNOW_ROUGH, NEW_SNOW_ALB, SNOW_ALB_ACCUM_A, SNOW_ALB_ACCUM_B, SNOW_ALB_THAW_A, root_depth, lai_djf, lai_son, alb_mam, alb_jja, Rarc, RGL, Sol_Atn, Trunk_ratio
SWE	SNOW_ROUGH, NEW_SNOW_ALB, SNOW_ALB_THAW_A, TEMP_TH1	ds, dsmax, ws, c, depth3, INFIL, watn, ks, depth2, bd, sdens, wcr, wpwp, resid_moist, GLAC_ALB, GLAC_ROUGH, GLAC_REDF, root_depth, root_fract1, root_fract2, alb_dja, alb_jja, alb_son, Rarc, Rmin, RGL,	PGRAD, T_LAPSE, depth1, SNOW_ALB_ACCUM_A, SNOW_ALB_ACCUM_B, SNOW_ALB_THAW_B, TEMP_TH_2, lai_djf, lai_mam, lai_jja, lai_son, alb_mam, Sol_Atn, Trunk_ratio

3.1 Informative parameters for streamflow

The soil parameters *ds*, *dsmax*, *ws*, *depth3*, *depth1* are consistently identified as sensitive to streamflow (e.g., Demaria et al., 2007; Bennett et al., 2018; Gou et al., 2020) and this reflects the empirical nature of the runoff and baseflow processes that are fundamental in the VIC family of models. In addition to these parameters, the soil parameters soil bulk density (*bd*), soil particle density (*sdens*) and the residual moisture (*resid_moist*) are also identified as invariant-informative to streamflow in the study area.

Figure 3 presents the sensitivity of the 29 variant-sensitive parameters with respect to streamflow (Table 5). These parameters include the remaining soil parameters, climate, snow, and most of the vegetation parameters. The climate parameters *TEMP_TH_1 and TEMP_TH_2* (i.e., the rain/snow temperature threshold parameter 1 and 2) have different sensitivity patterns. The parameter *TEMP_TH_1* is found to be informative across all basins except in the arid basin BruneauR, which has the lowest snow index (0.38). The parameter *TEMP_TH_2* is informative only in sub-basins located in the interiors of the Fraser and Peace. *T_LAPSE* is informative in the snow-dominated basins of the Fraser and the Columbia. The snow-related

parameters show different spatial sensitivity. For instance, *SNOW_ROUGH* is sensitive over all basins except for some snow-dominated basins of the Fraser and Columbia. The *NEW_SNOW_ALB* and *SNOW_ALB_THAW_A*, which control snow melt, are sensitive across all basins except the semi-arid basins of the Peace (north-east of the study region). Snowmelt in the study area contributes significantly to runoff, which explains the sensitivity of these parameters for streamflow. These results are consistent with the results found by Houle et al. (2017) who evaluated sensitivity of these parameters to snow water equivalent using the Sobol' method (Sobol', 1990).
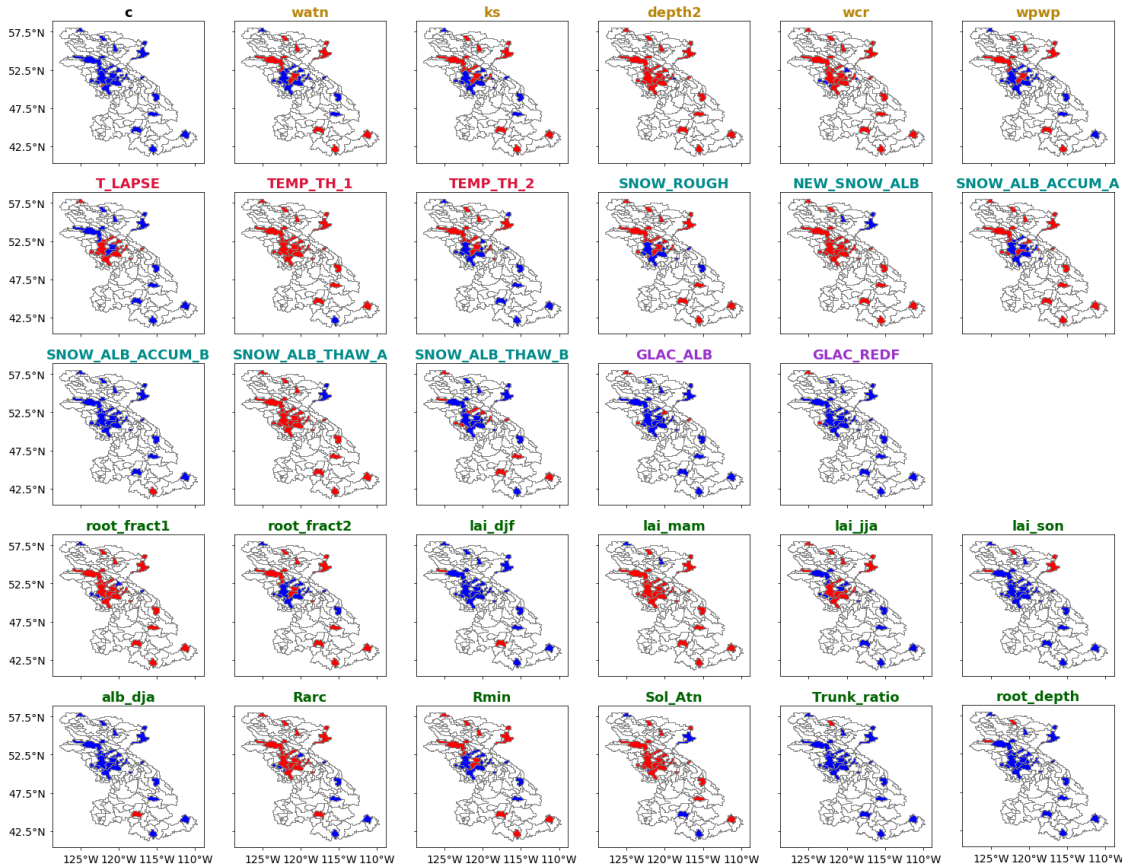
Figure 3: The spatial sensitivity of the 29 streamflow variant-informative parameters with red being informative and blue non-informative over the 25 selected basins. The nine invariant informative and six invariant non-informative parameters are not included.

In the semi-arid and arid basins, the exponent in Campbell's equation for hydraulic conductivity (*watn*), the saturated hydrologic conductivity (*ks*), and fractional soil moisture content at the wilting point (*wpwp*) are informative for streamflow. The *wpwp* parameter dictates baseflow estimation with the Arno model formulation (Francini and Pacciani, 1991) used in VIC (Gao et al., 2009). Given the limited precipitation in these basins, baseflow may be a significant streamflow source that explains the importance of this parameter in these basins. The root depth of the third layer (*root_depth*) is sensitive in the northern semi-

arid basins (NAUTL, HRNFC). The root fraction of the first layer (*root_fract1*) is sensitive in Columbia basins and the non-glacierized basins of the Fraser and Peace. The root fraction in the second layer (*root_fract2*) is sensitive only in the semi-arid and arid basins. The sensitivity of the LAI parameters is seasonal with springtime LAI being sensitive in almost all basins. For the glacierized headwater catchments the albedo of the glacier surface (*GLAC_ALB)* is informative for streamflow. The importance of this parameter increases with the basin glacier area and this parameter is influential in the four basins CLEAO, KWRNW, DONAL, and TASEK with the largest glacier area (between 115 km^2 and 194 km^2, between 7 % and 11 % of watershed area). The remaining glacierized basins have much smaller glacier areas (less than 1.5 % of the watershed area). The *GLAC_REDF* parameter is informative for streamflow as well in the western-glaciated basins TASEK and KWRNW, where average annual temperature is negative. Glaciers behave as natural water reservoirs that provide streamflow through ice melt and temporary meltwater storage within the glacier during late summer (Marshall et al., 2011). For instance, in the upper Columbia, glaciers contribute up to 25 % and 35 % of streamflow in August and September respectively and up to 6 % to the annual streamflow (Jost et al 2012, Jiskoot and Muller, 2012).

3.2 Informative parameters for evapotranspiration

There are 13 invariant-informative parameters that affect evapotranspiration in the study region (see Fig. 2 and Table 5). These include parameters that control soil drainage (*wcr*, *wpwp*, *resid_moist*), and soil storage capacity (*bd*, *depth1* and *depth2*). The invariant-informative parameters also include the climate parameters *TEMP_TH_1*, *TEMP_TH_2* and vegetation parameters seasonal leaf area index (*lai_mam*, *lai_jja*), minimum stomatal resistance (*Rmin*), and root fraction (*root_fract1*, *root_fract2*). The VIC-GL model computes evapotranspiration as the sum of four types of evaporation; evaporation from the canopy layer, transpiration from all three soil layers, soil evaporation from the top soil layer, and evaporation/sublimation from the snow or glacier surface (Liang et al., 1994). The soil parameters affect the bare soil evaporation that occurs at the top thin layer. The leaf area index parameters govern the amount of water intercepted by the canopy, which controls canopy evaporation. Leaf area index and stomatal resistance (*Rmin*) influence the estimation of vegetation transpiration and the root fraction dictates the amount of transpiration from each soil layer (Gao et al., 2009). These parameters are defined for each land cover type in the vegetation library. They are typically fixed based on observed values, which ignores the large estimation and scaling uncertainties around their values (Mendoza et al., 2015). In this paper, the sampling of *LAI* and *Rmin* values is based on a perturbation of observed values (see Table 3; Type "Multiplicative factor"). The sensitivity of evapotranspiration to this perturbation illustrates the need to obtain accurate values for these parameters or consider their uncertainty in the model calibration process. The rain/snow temperature thresholds (*TEMP_TH_1*, *TEMP_TH_2*) are likely to impact the throughfall (water that penetrates a plant canopy) and rainfall/snow interception (rain captured, stored, and evaporated from the vegetation surface) (Levia et al., 2019).

371
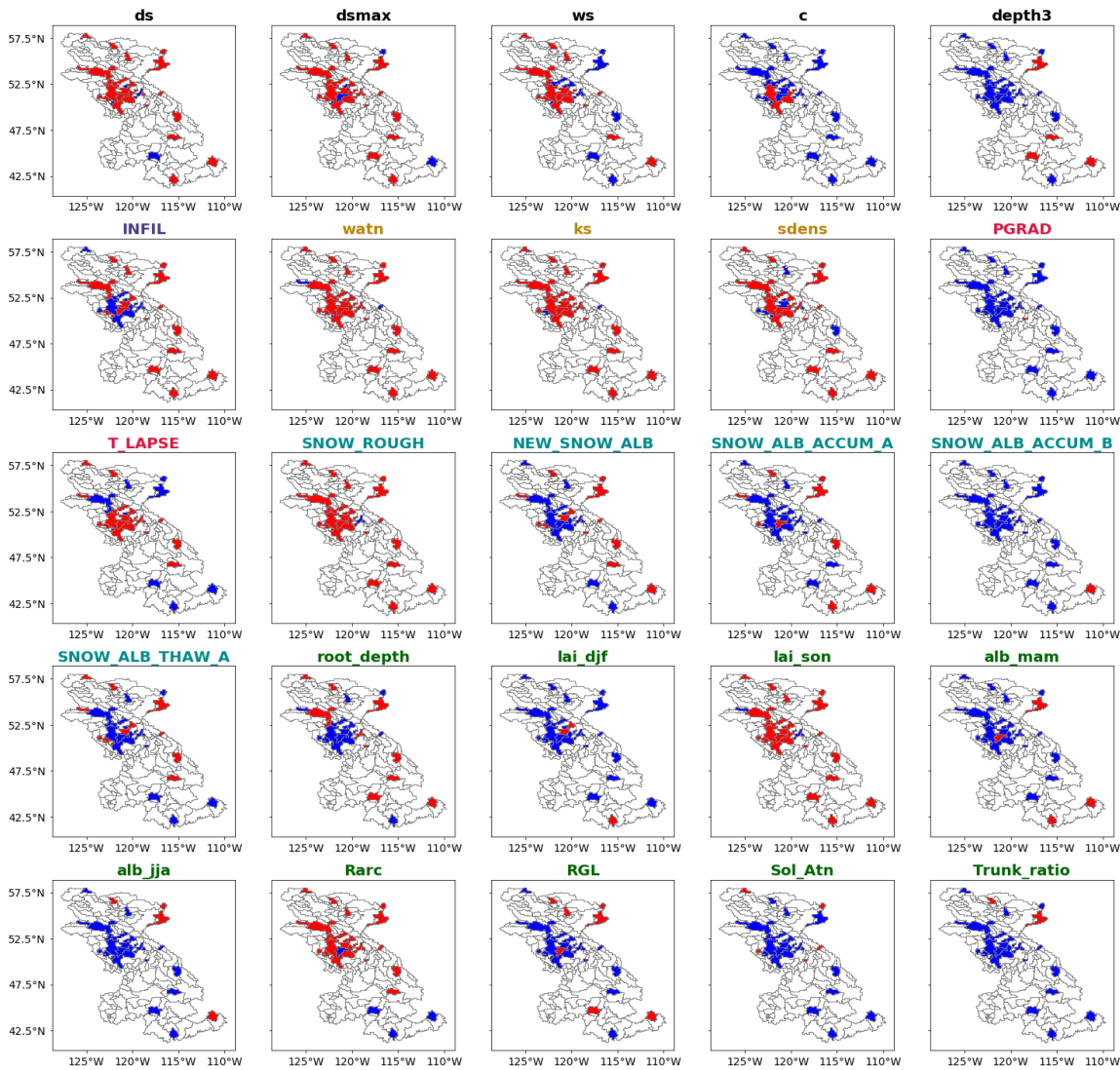
Figure 4: The spatial sensitivity of the 25 evapotranspiration variant-informative parameters with red being informative and blue non-informative over the 25 selected basins. The 13 invariant informative and 6 invariant non-informative parameters are not included. For the number of occurrences of informative parameters see Figure 2.

Table 5 lists the six invariant-noninformative parameters for evapotranspiration which are the glacier parameters, autumn and winter vegetation albedo, and the albedo decay exponent during the thaw period *SNOW_ALB_THAW_B*. Figure 4 presents the spatial sensitivity of the 25 variant-informative parameters with respect to evapotranspiration. Some parameters show a clear spatial pattern of sensitivity that is related to basin physical characteristics. For instance, *T_LAPSE* is sensitive in snow-dominated basins, whereas *INFIL* and *sdens* are sensitive in semi-arid and arid basins. The baseflow parameters (*ds*, *dsmax*) are informative in most basins while the parameter *ws* is only informative in humid sub-basins. The surface roughness of the

381   snowpack (*SNOW_ROUGH*), the architectural resistance of vegetation (*Rarc*), which affects the vertical wind profile, and

382   autumn leaf area index (*lai_son*) are also influential to evapotranspiration in most basins.

3.3 Informative parameters for snow water equivalent

384   Amongst the six snow-parameters, only three (*SNOW_ROUGH*, *NEW_SNOW_ALB*, *SNOW_ALB_THAW_A)* are invariant-

385   informative for snow water equivalent. The climate parameter *TEMP_TH_1* is also invariant-informative for snow water

386   equivalent. The parameter *TEMP_TH_2* is informative in the majority of the basins except in the semi-arid basins of the Peace.

387   The sensitivity of the remaining three snow parameters (*SNOW_ALB_ACCUM_A*, *SNOW_ALB_ACCUM_B*, *and*

388   *SNOW_ALB_THAW_B*) and the two climate parameters (*PGRAD*, *T_LAPSE*) varies within the study region. Figure 5 presents

389   the sensitivity of the 14 variant-informative parameters for snow water equivalent. The *T_LAPSE* and *PGRAD* are sensitive in

390   the high-altitude basins. The parameter *SNOW_ALB_ACCUM_B* is informative in the basins of the Columbia and Peace, and

391   in the semi-arid basins of the Fraser. The sensitivities of seasonal leaf area index (*lai_djf*, *lai_mam*, *lai_jja*, and *lai_son*), ratio

392   of total tree height that is trunk (*Trunk_ratio*), and the solar attenuation factor (*Sol_Atn*) show a clear spatial pattern. These

393   parameters are informative in basins where forest is the dominant land cover (i.e., Fraser and Peace). The springtime vegetation

394   albedo (*alb_mam*) is sensitive over the snow-dominated basins. The sensitivity of snow water equivalent for vegetation

395   parameters can be explained by the impact of forest cover on snow accumulation and ablation processes, mainly by snowfall

396   interception and modification of incoming radiation and wind speed below the forest canopy (Andreadis et al., 2009). These

397   finding are consistent with those of Houle et al., (2017) and Bennett et al., (2018).

398
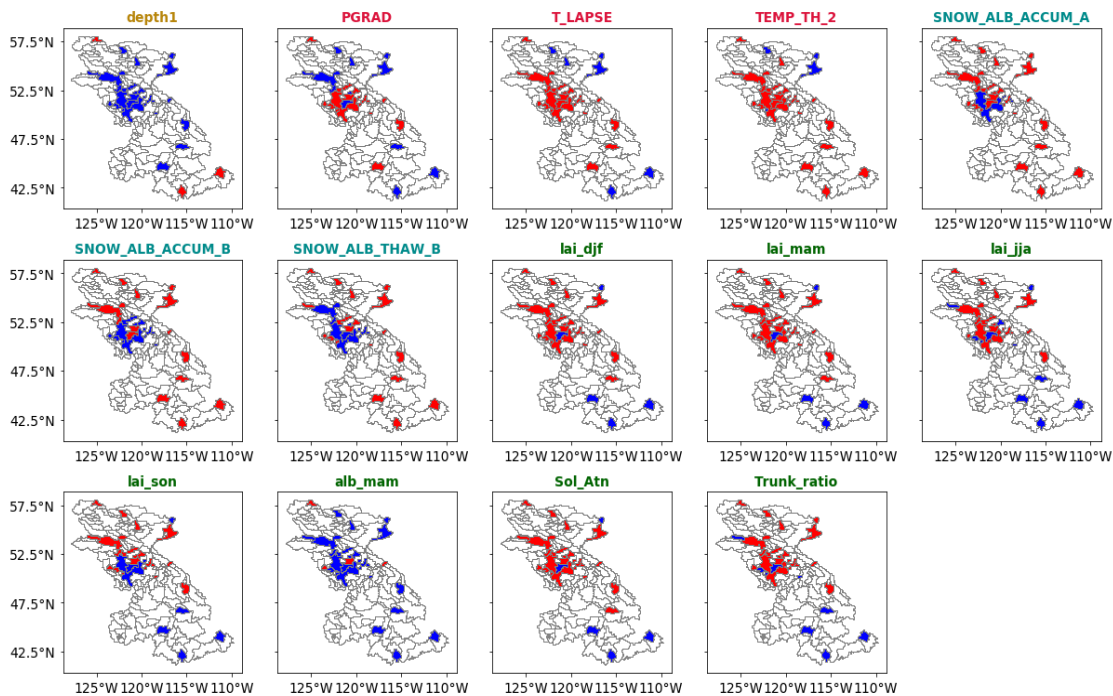
Figure 5: The spatial sensitivity of the14 snow water equivalent variant-informative parameters with red being informative and blue non-informative over the 25 selected basins. The 4 invariant informative and 26 invariant non-informative parameters are not included. For the number of occurrences of informative parameters see Figure 2.

3.4 Watershed classification

Figure 6 presents the dendogram, a diagram tree of clusters resulting from the agglomerative hierarchical clustering using climate indices and the combination of climate indices and vegetation class cover. Clustering based on climate indices yields four clusters whereas clustering based on climate indices and vegetation cover results in five clusters.
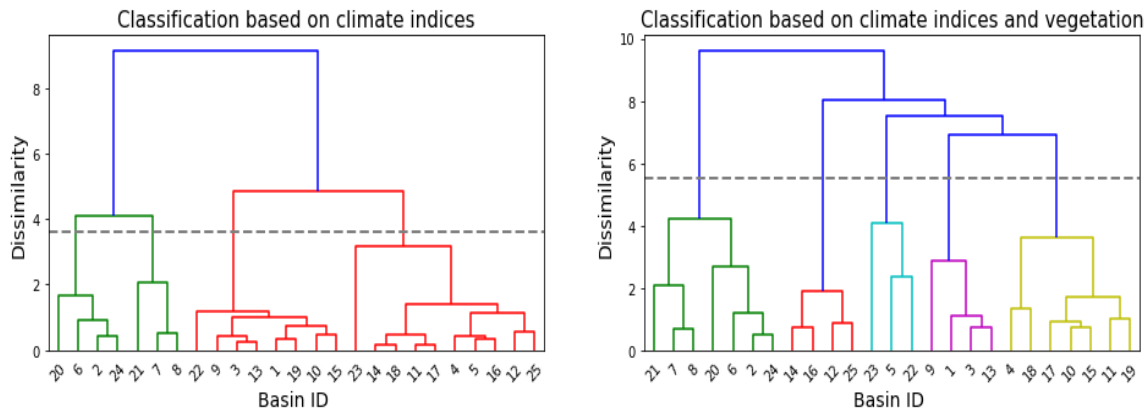
408

409 **Figure 6: Watershed classification dendogram using climate indices and the combination of climate and vegetation indices. The**
410 **height of each node represents the distance between its branches and the dashed line represents the cutoff threshold to distinguish**
411 **the 4 clusters in the case of climate-based classification and 5 clusters in the case of climate-land cover-based classification. The**
412 **threshold is chosen as a trade-off between cluster dissimilarity and within cluster variance.**

413

414   Figure 7 shows the results of the hierarchical clustering analyses and Fig. 8 and 9 present the attribute statistics for each cluster.

415   The clusters produced using climatic attributes can be described as follows. Cluster #1 consists of dry basins located in the

416   southern Columbia, eastern Peace, and central Fraser basins. Cluster #2 contains glacierized watersheds along the Coast

417   Mountains and the Rocky Mountains. Cluster #3 contains semi-arid basins in the interior Fraser and eastern Columbia, and

418   cluster #4 contains snow-dominated basins with very low glacier area (less than 4 % of watershed area) compared to cluster

419   #2. Clusters obtained using both climatic and vegetation attributes correspond to clusters based on climate that were merged

420   or divided based on vegetation class cover dominance. Cluster #1 contains all glaciered watersheds and corresponds to clusters

421   #2 and #4 obtained with climatic based clustering. Cluster #2 consist of dry basins dominated by land cover 11 (temperate or

422   sub-polar shrubland) that are located in the southern Columbia basin. Cluster #3 consist of dry basins dominated by land cover

423   9 (i.e., mixed forest) located in the eastern Peace River basin. Cluster #4 represents arid basins in the interior Fraser and upper

424   Columbia dominated by land cover 2 (i.e., temperate or sub-polar needleleaf forest - high-elevation) and cluster #5 consists of

425   wet basins dominated with land cover 4 (i.e., temperate or sub-polar needleleaf forest - coastal/humid/dense).
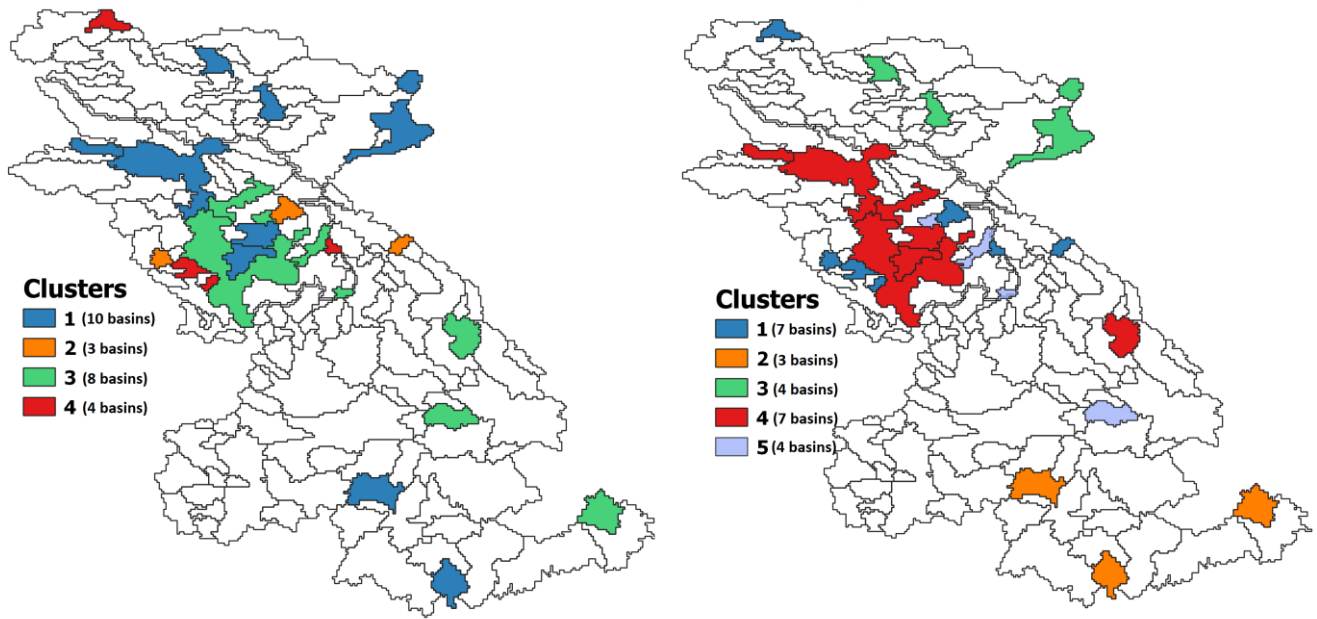
426

427 **Figure 7: Map of clusters obtained using only climatic attributes (left), and using both vegetation- and climatic attributes (right).**
428

429

430
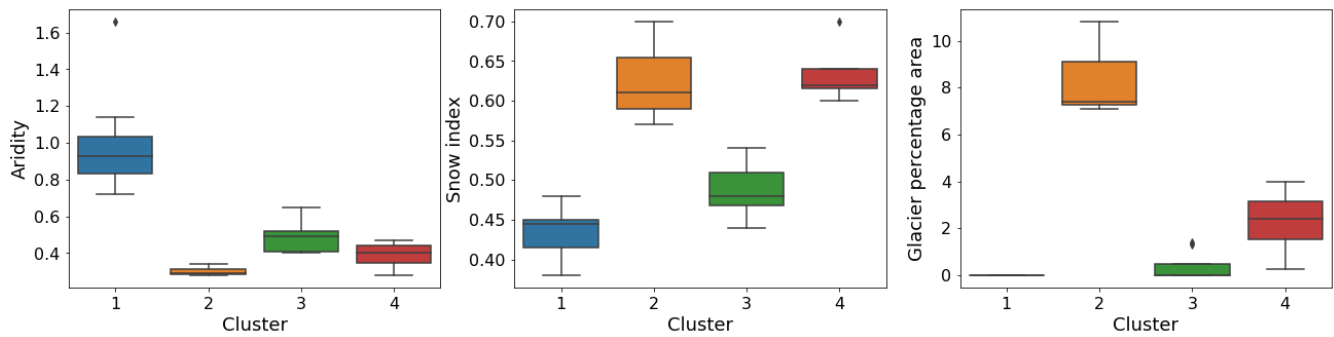
431

432 **Figure 8: Box-plots of the climate attributes for each cluster produced by climate based classification.**

433

434
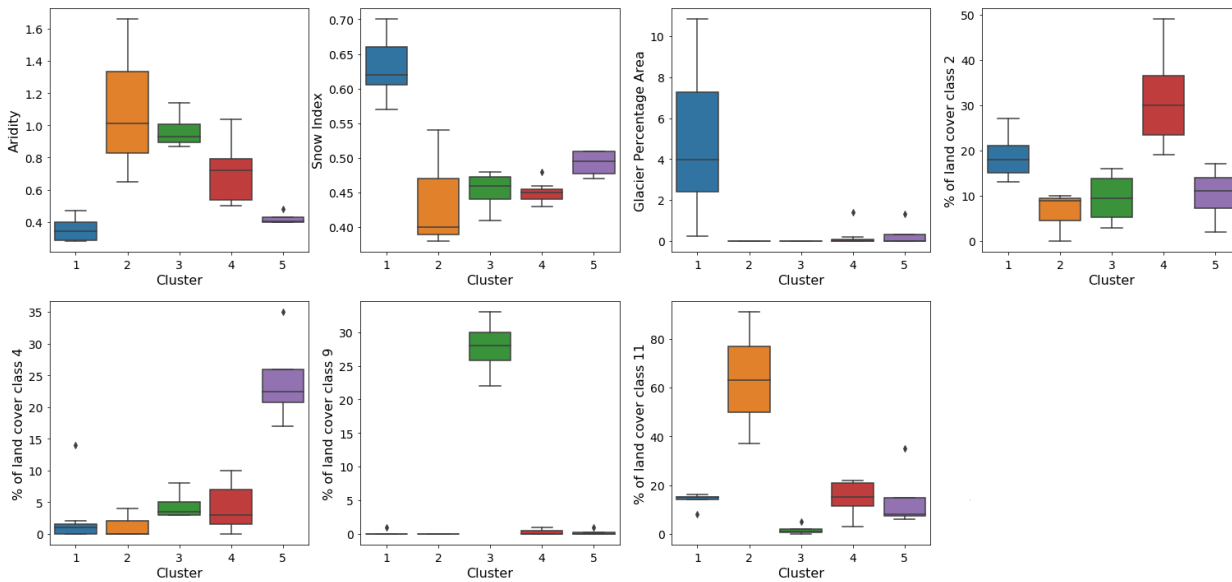
Figure 9: Box-plots of attributes of each cluster produced by climate- and vegetation-based classification.

436

3.5 Watershed classification as a way to transfer parameter sensitivity

The distribution of *F1* scores obtained by transferring informative parameters for streamflow, evaporation and snow water equivalent using both clustering analyses and a range of donor basins is presented in Fig. 10. The *F1* scores calculated for transferring streamflow informative parameters based on climatic attributes range between 0.66 (using 9 donor basins) and 0.98 (using between three to seven donor basins), whereas this score ranges between 0.65 (using six donor basins) and 0.96 (using six donor basins) when using both climate and vegetation attributes. For evapotranspiration the *F1* scores obtained by climatic based clustering range between 0.63 (using six donor basins) and 0.96 (using three to six donor basins). The scores range between 0.7 (using two donor basins) and 0.95 (using a single donor basin) when using both climatic and land cover attributes for clustering analysis. The *F1* scores for snow water equivalent range between 0.83 (using four to nine donor basins) and 1 (using one to two donor basins) when transferring informative parameters based on climatic attributes and the combination of climatic attributes and vegetation.
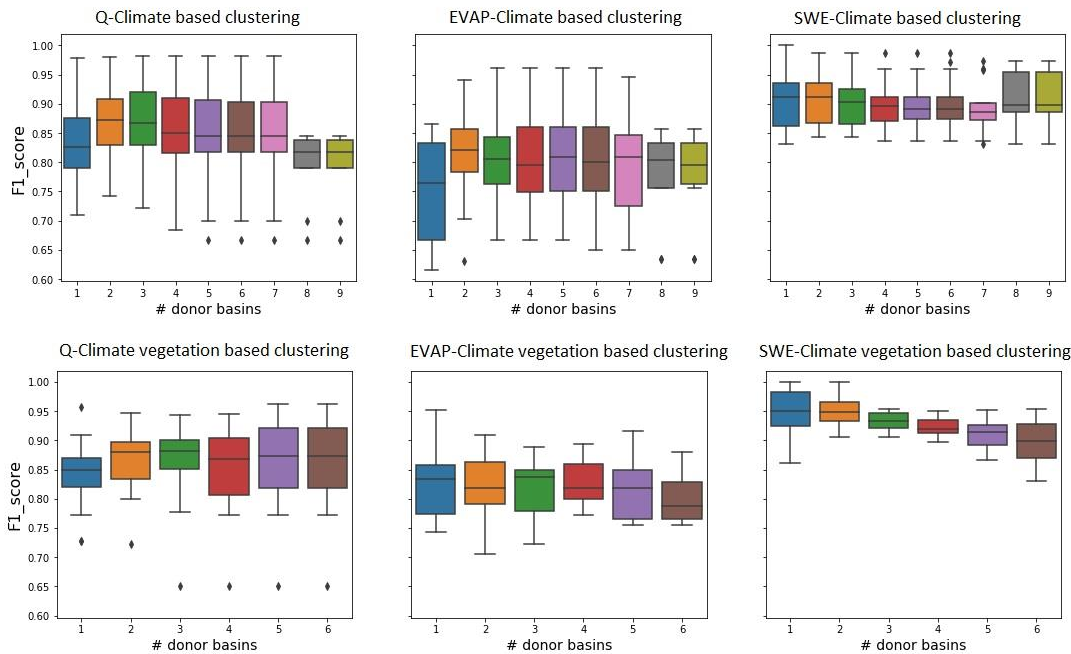
Figure 10: *F1 score distribution obtained by transferring informative parameters over the 25 basins.*

Transferring informative parameters based on more than a single donor basin improves the *F1* score except when transferring evapotranspiration informative parameters using climatic and vegetation clustering analysis. Overall, the results shows that two donor basins would be sufficient to generalize informative parameters to each cluster. Therefore, for each model output we compare the *F1* distributions using two donor basins based on both clustering analysis with the Wilcoxon test. The p-value of the test applied to *F1* score distributions obtained by transferring streamflow informative parameters is 0.49 and by transferring evapotranspiration informative parameters is 0.48. Hence, the *F1* score distributions using climatic clustering analysis and climatic-land cover analysis are not significantly different. Therefore, using only climatic attributes would be sufficient to transfer informative parameters to streamflow and evapotranspiration. These findings are consistent with other VIC studies (Demaria et al., 2007) and for other hydrologic models (e.g., Rosero et al., 2010) showing that parameter sensitivity for streamflow can be transferred based predominantly on climate similarity.

The Wilcoxon test statistic applied to the *F1* distribution resulting from transferring snow water equivalent informative parameters is 31 with a p-value of 0.0006. This suggests that there is a significant improvement when using both climatic and land cover attributes to transfer snow water equivalent parameter sensitivity. The importance of land cover and vegetation properties as a control on snow accumulation and ablation is consistent with previous studies (e.g., Bennett et al., 2018).

4 Discussion

In this work, we have examined the sensitivity of an extensive list of VIC parameters to streamflow, evapotranspiration, and snow water equivalent over 25 basins spanning a range of hydroclimatic conditions. We found that informative parameters vary spatially with climate and land cover depending on the model output considered. The findings are in line with previous VIC sensitivity analysis studies (e.g., Demaria et al., 2007; Bennett et al., 2018; Gou et al., 2020, Sepúlveda, 2021). In addition, the two climate parameters temperature lapse rate (*T_LAPSE*) and the precipitation gradient (*PGRAD*) omitted in previous studies have been found to be informative to headwater glacierized watersheds and snow dominated non-glacierized watersheds. The *T_LAPSE* parameter is typically fixed when developing gridded meteorological data. For instance, Bohn et al., (2016) used a gridded temperature corrected with a lapse rate of 6.5 °K/km to force VIC over southwestern US and northwestern Mexico. However, several studies have indicated that the often-used constant lapse rates 6-6.5 °C/km are not representative of the surface conditions over different mountainous regions and may differ for each slope within the same mountain (Blandford et al., 2008; Minder et al., 2010, Córdova et al., 2016).

In this study, we showed that watershed classification helps identify spatial patterns of informative parameters at a reduced cost. Hence, it reduces the cost of performing sensitivity analysis at the same scale of large-scale land surface models. In our case, watershed classification based on climatic attributes (snow and aridity index) and percentage of glacier area was sufficient to transfer parameter sensitivity between basins of similar attributes. However, incorporating vegetation class cover significantly improved the identification of sensitive parameters for snow water equivalent. The results show that two donor basins per cluster are sufficient to identify sensitive parameters. These results imply that the cost of running sensitivity analysis over a large domain encompassing N clusters of basins would be reduced to the cost of running 2N sensitivity analyses. The information gained can then be extrapolated to large domain based on sub-watershed membership to the N clusters. Thus, candidate parameters for model calibration can be identified at a substantially reduced computational cost as compared to running a large-domain sensitivity analysis. For example, climatic based classification of the 158 basins that covers the entire domain results in four watershed clusters (see Fig. 11) as follows. Cluster #1 consist of glaciered basins along the Coast Mountains and Rocky Mountains. Cluster #2 groups dry basins located in interior and southern Columbia, eastern Peace, and upper Fraser basins. Cluster #3 contains snow-dominated basins in north Peace River basin and eastern Columbia River basin whereas Cluster #4 contains rainfall dominated basins in western Columbia River basin. These clusters are consistent with the clusters obtained by classifying the 25 basins except for cluster #4 because the sample of the studied basins does not include any rainfall-dominated basins. Hence, the cost of performing a sensitivity analysis across the 158 basins is reduced to the cost of evaluating parameter sensitivity over eight basins (i.e., two basins for each basin cluster).

494
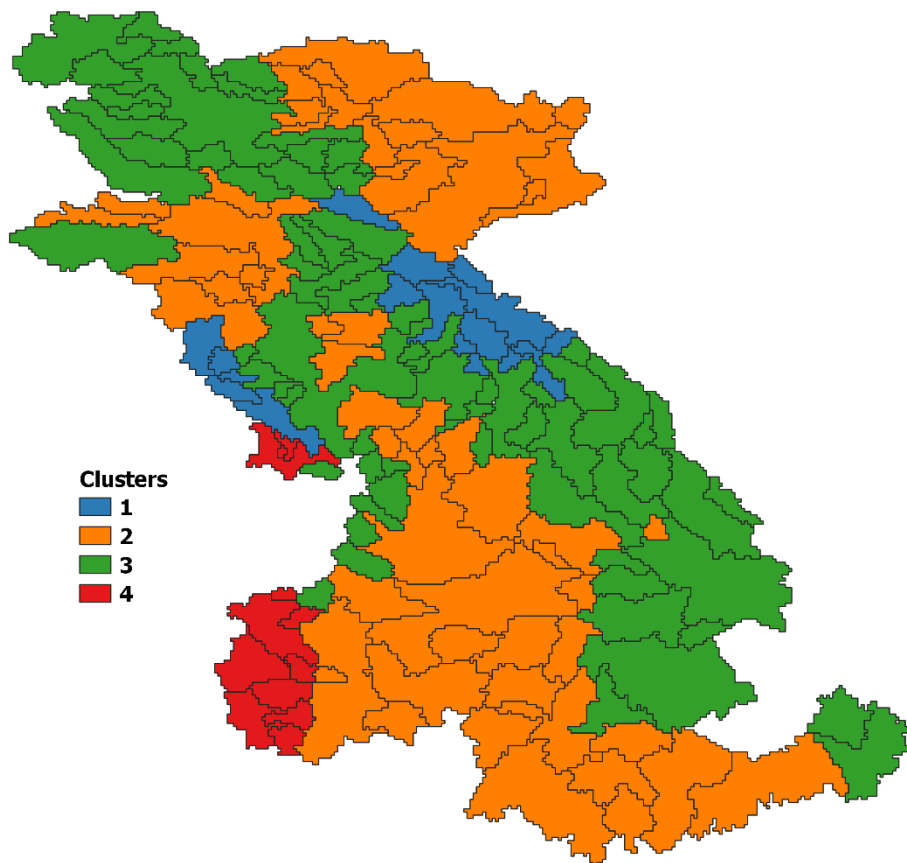
Figure 11: Climatic based classification of the 158 sub-basins of the Peace River, Fraser River, and Columbia River basins.

496

497 It has been argued in the literature that calibration based solely on streamflow is not sufficient to ensure model accuracy and

498 fidelity (Rakovec et al., 2016). To improve model realism, recent calibration strategies follow a process-based approach. This

499 approach relies either on adjusting model parameters against hydrological signatures extracted from streamflow timeseries that

500 link to the underlying model processes (Yilmaz et al., 2008; Euser et al., 2013, Shafii and Tolson; 2015; Rakovec et al., 2016),

501 against measurements of different model outputs such as evapotranspiration, snow cover, and baseflow (e.g., Isenstein et al.,

502 2015, Ismail et al., 2020), or by hydrograph decomposition (e.g., He et al., 2015, Shafii et al., 2017; Larabi et al., 2018).

503 However, we recognize that the effort to constrain multiple hydrologic processes will require a substantial increase in the size

504 of the parameter domain during model calibration. For instance, our sensitivity analysis results from Table 5 and Fig. 12

505 suggest that calibrating VIC-GL in a multi-objective/multi-variable framework would require a high number of parameters in

506 the calibration process (30 to 38 parameters depending on the sub-basin if one is to consider all informative parameters for

507 each output considered here). Across the 25 sub-basins, an average of 77 % of parameters (34 of 44 parameters analyzed) are

508 informative to at least one of simulated streamflow, evapotranspiration, or snow water equivalent (see Fig. 12). This contrasts
509 with previous studies that typically calibrate fewer than 12 VIC parameters (e.g., Troy et al., 2008; Isenstein et al., 2015;
510 Mizukami et al., 2017; Rakovec et al., 2019; Ismail et al., 2020). Options to tackle this more complex calibration problem are
511 not evaluated here but could include suitable one-step multi-objective optimization algorithms such as PADDS (Asadzadeh et
512 al. (2014)), or a stepwise multi-objective calibration approach where each set of informative parameters for a specific flux are
513 adjusted separately (Larabi et al., 2018). Another approach to reduce the complexity of the calibration problem would be to
514 use a smaller parameter range, which could speed the convergence rate of the search algorithm to the optimal solution.
515 However, this would have to be done carefully, possibly utilizing expert knowledge, in order to ensure the narrower range still
516 contains the optimal solution (Mai, 2023).

517

518
519 **Figure 12: Informative parameters (blue) for at least one of simulated streamflow, evapotranspiration, and snow water equivalent.**
520 **Basin ID description is provided in Table 1.**

521

522

523

In previous VIC applications, the same parameters are adjusted over large domains to fit the model to streamflow (e.g., Nijssen et al., 2001; Obeidillah et al., 2014; Xue et al., 2015, Mizukami et al., 2017) and against other model output (Isenstein et al., 2015; Ismail et al., 2020) ignoring both the spatial variability of parameter sensitivity and dependence of parameter sensitivity to the hydrological processes. To account for this spatial variability, a multi-site cascading approach (Xue et al., 2015) where calibration parameter selection varies depending on the site can be used. Overall, there remains a need to study how information regarding the spatial variability and process dependence of parameter sensitivity is best integrated into a multi-variable parameter estimation framework.

In this study, the low-cost EEE sequential screening method (Cuntz et al., 2105) was used to identify informative parameters. However, this method does not quantitatively rank the importance of these informative parameters. In situations where it is desired to reduce the number of calibration parameters below the counts identified by EEE analyses, a quantitative approach such as variance-based methods (e.g., Sobol', 1990; Saltelli, 2002) or qualitative approach that provides parameter groupings based on their sensitivity could be considered (Sheikholeslami et al., 2019; Mai et al., 2020, 2022). However, future work is required to determine the conditions under which a reduction in the number of calibrated parameters (i.e., by not calibrating some parameters that are informative) could potentially yield better calibration results, particularly in a multi-objective context.

5 Conclusions

Land surface models tend to have large numbers of parameters, many of which cannot be measured directly. Sensitivity analysis is therefore often employed to identify parameters with significant impact on model output variance. Performing sensitivity analysis for large-scale land surface models is, however, computationally demanding. In this study, we consider whether computational cost can be reduced by using watershed classification to transfer information about which parameters sensitively affect streamflow, evapotranspiration and snow water equivalent between basins that have similar climatic and vegetation land cover attributes.

The study was performed using a large domain implementation of a hydrologic model as an example. Specifically, we used an updated version of the VIC model (Schnorbus, 2018) that has been coupled to a regional glacier model and implemented across a very large domain in the Pacific Northwest region of North America. A wide range of VIC model parameters was evaluated that include five baseflow parameters, one runoff parameter, nine drainage parameters, four climate parameters, six snow-related parameters, three glacier parameters, and 17 vegetation related parameters. The sensitivity analysis was performed over 25 basins spanning a range of hydroclimatic conditions to understand the spatial variability of parameter sensitivities with regard to streamflow, evapotranspiration and snow water equivalent. Parameter sensitivities for each model output were found to vary in a predictable way with basin climate and land cover characteristics.

553 Watershed classification was employed to classify the 25 basins into homogenous groups based on climatic attributes (aridity
554 and snow index) and percentage of glacier area and vegetation land cover. This classification was used to transfer sensitive
555 parameters to each basin based on its group membership. This approach was shown to be able to efficiently identify sensitive
556 parameters with a median *F1* score of 0.87 for streamflow, 0.83 for evapotranspiration and 0.95 for snow water equivalent.
557 These findings suggest that parameter sensitivity can be performed by classifying watersheds into broad groups and then
558 analyzing sensitivity for only a subset of the basins in each group. In our large domain example, we found that it would likely
559 be sufficient to perform sensitivity analysis in 4 % (or fewer) of the basins contained within the domain. This would
560 substantially reduce the cost of the sensitivity analyses that are used to determine the model calibration strategy, or for a given
561 computing budget, would enable the consideration of a broader range of parameters than could be considered if sensitivity
562 analysis were to be performed across the entire domain.

563 The parameter classification based on parameter sensitivities informs which parameters should be adjusted (invariant-
564 informative and variant-informative) depending on the calibration variables that are considered and the local climatic
565 conditions. We found that for a multi-variable calibration approach targeting streamflow, evapotranspiration and snow water
566 equivalent, an average of 77 % of VIC parameters (i.e., 34 of 44 parameters analyzed) were identified as calibration candidates.
567 These parameters include not only those that control runoff and baseflow generation, but also parameters that control snow
568 processes and describe vegetation properties. The findings of this study highlight the need to explore efficient ways to decrease
569 the complexity of multi-process-based calibration of land surface models arising from the increased dimensionality of both the
570 parameter and objective function spaces.

571 Finally, we note that more specific modelling objectives, such as the skillful representation of peaks flows (for flood forecasting
572 purposes), or low flows (for predicting summer drought impacts) could also be considered using the approach that has been
573 proposed. Similarly, the results and methods are applicable to other land surface models.

574 **Code availability**

575 Code of Efficient Elementary Effects (EEE) method is freely available with documentation and examples at
576 https://doi.org/10.5281/zenodo.3620895

577 **Author contributions**

578 The study conception was performed by SL, MS and FZ. Sensitivity analysis methodology and code were handled by JM.
579 Formal analysis, investigation and writing original draft were performed by SL. All authors contributed to the writing-review
580 and editing of the manuscript.
581

Competing interests

The authors declare that they have no conflict of interest.

Acknowledgments

Financial support from the Canada First Research Excellence Fund and the Global Water Futures (GWF) program is gratefully acknowledged.

References

Andreadis, K., Storck, P., and Lettenmaier, D. P.: Modeling snow accumulation and ablation processes in forested environments, Water Resour. Res., 45, W05429, doi:10.1029/2008WR007042, 2009.

Asadzadeh, M., Tolson, B. A., and Burn, D. H.: A new selection metric for multiobjective hydrologic model calibration, Water Resour. Res., 50, 7082–7099, doi:10.1002/2013WR014970, 2014.

Bao, Z., Zhang, J., Liu, J., Fu, G., Wang, G., He, R., Yan, X., Jin, J., and Liu, H.: Comparison of regionalization approaches based on regression and similarity for predictions in ungauged catchments under multiple hydro-climatic conditions, J. Hydrol., 466–467(1), 37–46, 2012.

Baret, F., Weiss, M., Lacaze, R., Camacho, F., Makhmara, H., Pacholcyzk, P., and Smets, B.: GEOV1: LAI and FAPAR essential climate variables and FCOVER global time series capitalizing over existing products. Part1: Principles of development and production, Remote Sens. Environ., 137, 299– 309, doi:10.1016/j.rse.2012.12.027, 2013.

Beck, H. E., Van Dijk, A. I. J. M., De Roo, A., Miralles, D. G., McVicar, T. R., Schellekens, J., and Bruijnzeel, L. A.: Global-scale regionalization of hydrologic model parameters, Water Resour. Res., 52, 3599–3622, doi:10.1002/2015WR018247, 2016.

Bennett, K. E., Werner, A. T., and Schnorbus, M.: Uncertainties in Hydrologic and Climate Change Impact Analyses in Headwater Basins of British Columbia, Journal of Climate, 25, 5711–5730, https://doi.org/10.1175/JCLI-D-11-00417.1, 2012.

Bennett, K. E., Urrego Blanco, J. R., Jonko, A., Bohn, T. J., Atchley, A. L., Urban, N. M., and Middleton, R. S.: Global sensitivity of simulated water balance indicators under future climate change in the Colorado Basin, Water Resources Research, 54, 132–149. https://doi.org/10.1002/ 2017WR020471, 2018.

Blandford, T., Humes, K., Harshburger, B., Moore, B., Walden, V., and Ye H.: Seasonal and synoptic variations in near-surface air temperature lapse rates in a mountainous basin, J. Appl. Meteorol. Climatol., 47(1), 249–261, doi:10.1175/2007JAMC1565.1, 2008.

610 Bohn, T. J., and Vivoni, E. R.: Process-based characterization of evapotranspiration sources over the North American monsoon

611   region, Water Resources Research, 52, 358–384. https://doi.org/10.1002/2015WR017934, 2016.

612 Boscarello, L., Ravazzani, G., Cislaghi, A. and Mancini, M.: Regionalization of Flow-Duration Curves through Catchment

613   Classification with Streamflow Signatures and Physiographic-Climate Indices, J. Hydrol. Eng., 21(3), doi:

614   10.1061/(ASCE)HE .1943-5584.0001307, 2016.

615 Camacho, F., J. Cernicharo, R. Lacaze, F. Baret, and Weiss, M.: GEOV1: LAI, FAPAR essential climate variables and

616   FCOVER global time series capitalizing over existing products. Part 2: Validation and intercomparison with reference

617   products, Remote Sens. Environ., 137, 310–329, doi:10.1016/j.rse.2013.02.030, 2013.

618 Campolongo, F., Cariboni, J., and Saltelli, A.: An effective screening design for sensitivity analysis of large models, Environ.

619   Model. Softw., 22, 1509–1518, doi: https://doi.org/10.1016/j.envsoft.2006.10.004, 2007.

620 Cherkauer, K. A., Bowling, L. C., and Lettenmaier, D. P.: Variable infiltration capacity cold land process model updates, Glob.

621   Planet. Change, 38, 151–159, doi: 10.1016/S0921-8181(03)00025- 0, 2003.

622 Choudhury, B. J., and Monteith, J. L.: A four-layer model for the heat budget of homogeneous land surfaces, Q. J. R. Meteorol.

623   Soc., 114, 373–398, doi:10.1002/qj.49711448006, 1988.

624 Chicco, D. and Jurman, G.: The advantages of the Matthews correlation coefficient (MCC) over F1 score and accuracy in

625   binary classification evaluation, BMC Genomics, 21:6, doi: https://doi.org/10.1186/s12864-019-6413-7, 2020.

626 Córdova, M., Célleri, R., Shellito, C.J. et al.: Near-surface air temperature lapse rate over complex terrain in the Southern

627   Ecuadorian Andes: implications for temperature mapping, Arctic, Antarctic, and Alpine Research, 48, No.4, pp. 673–684,

628   doi: http://dx.doi.org/10.1657/AAAR0015-077, 2016.

629 Compo, G. P., and Coauthors: The Twentieth Century Reanalysis Project, Q. J. R. Meteorol. Soc., 137, 1–28, doi:

630   https://doi.org/10.1002/qj.776, 2011.

631 Cuntz, M., et al. Computationally inexpensive identification of noninformative model parameters by sequential screening,

632   Water Resour. Res., 51, 6417–6441, doi: 10.1002/2015WR016907, 2015.

633 Cuntz, M., Mai, J., Samaniego, L., Clark, M., Wulfmeyer, V., Branch, O., Attinger, S., and Thober, S.: The impact of standard

634   and hard-coded parameters on the hydrologic fluxes in the Noah-MP land surface model, J. Geophys. Res. Atmos., 1-25,

635   doi: http://doi.org/10.1002/(ISSN)2169-8996, 2016.

636 Danielson, J. J., and Gesch, D. B.: Global Multi-resolution Terrain Elevation Data 2010 (GMTED2010), U.S. Geological

637   Survey, Reston, Virginia, http://pubs.usgs.gov/of/2011/1073/pdf/of2011-1073.pdf (Accessed November 2, 2015), 2011.

638 Demaria, E. M., Nijssen, B., and Wagener, T.: Monte Carlo sensitivity analysis of land surface parameters using the Variable

639   Infiltration Capacity model, J. Geophys. Res., 112, D11113, doi:10.1029/2006JD007534, 2007.

640 Demirel, M. C., Mai, J., Mendiguren, G., Koch, J., Samaniego, L., and Stisen, S.: Combining satellite data and appropriate

641   objective functions for improved spatial pattern performance of a distributed hydrologic model, Hydrology and Earth

642   System Sciences, 22(2), 1299–1315, doi: http://doi.org/10.5194/hess-22-1299-2018, 2018.

643 Devak, M. and Dhanya, C.T.: Sensitivity analysis of hydrological models: review and way forward, Journal of Water and
644   Climate Change, doi: 10.2166/wcc.2017.149, 2017.

645 Dickinson, R. E.: Land surface processes and climate - surface albedos and energy balance, Theory of Climate, B. Saltzman,
646   Ed., Vol. 25 of Advances in Geophysics, Academic Press, Inc., New York, NY, 305–353, 1983.

647 Ducoudré, N. I., Laval, K., and Perrier A.: SECHIBA, a New Set of Parameterizations of the Hydrologic Exchanges at the
648   Land-Atmosphere Interface within the LMD Atmospheric General Circulation Model, J. Clim., 6, 248–273,
649   doi:10.1175/1520- 0442(1993)0062.0.CO2, 1993.

650 Euser, T., Winsemius, H.C., Hrachowitz, M., Fencia, F., Uhlenbrook, S. and Savenije, H.H.G.: A framework to assess the
651   realism of model structures using hydrological signatures, Hydrol. Earth Syst. Sci., 17, 1893-1912, 2013.

652 Fitzpatrick, N., Radić, V., and Menounos, B.: A multi-season investigation of glacier surface roughness lengths through in situ
653   and remote observation. The Cryosphere, 13, 1051–1071, doi: https://doi.org/10.5194/tc-13-1051-2019, 2019.

654 Francini, M., and Pacciani, M.: Comparative-analysis of several conceptual rainfall runoff models, Journal of Hydrology,
655   122(1-4), 161-219, 1991.

656 Gao, H. et al.: Water Budget Record from Variable Infiltration Capacity (VIC) Model, In Algorithm Theoretical Basis
657   Document for Terrestrial Water Cycle Data Records (unpublished), 2009.

658 Garambois, P. A., Roux, H., Larnier, K., Labat, D., and Dartus, D.: Parameter regionalization for a process-oriented distributed
659   model dedicated to flash floods, J. Hydrol., 525, 383–399, doi: 10.1016/j.jhydrol.2015.03.052, 2015.

660 Grenfell, T. C.: Albedo, Encyclopedia of Snow, Ice and Glaciers, V.P. Singh, P. Singh, and U.K. Haritashya, Eds., Springer
661   Netherlands, 23–35, 2011.

662 Göhler, M., Mai, J., and Cuntz, M.: Use of eigen decomposition in a parameter sensitivity analysis of the Community Land
663   Model, Journal of Geophysical Research: Biogeosciences, 118(2), 904–921, doi: http://doi.org/10.1002/jgrg.20072, 2013.

664 Gou, J., Miao, C., Duan, Q., Tang, Q., Di, Z., Liao, W., et al.: Sensitivity analysis-based automatic parameter calibration of
665   the VIC model for streamflow simulations over China, Water Resources Research, 56, e2019WR025968, doi:
666   https://doi.org/10.1029/2019WR025968, 2020.

667 Hamlet AF, and Lettenmaier. DP.: Effects of climate change on hydrology and water resources in the Columbia River Basin,
668   Journal of the American Water Resources Association, 35,6, 1999.

669 He, Y., Bardossy, A. and Zehe, E.: A review of regionalisation for continuous streamflow simulation, Hydrol. Earth Syst. Sci.,
670   15, 3539–3553, doi: 10.5194/hess-15-3539-2011, 2011.

671 He, R., and Pang B.: Sensitivity and uncertainty analysis of the Variable infiltration Capacity model in the upstream of Heihe
672   River basin, Proc. Int. Assoc. Hydrol. Sci., 8 (4), 312–316, doi: https://doi.org/10%20.2166/wcc.2017.149, 2014.

673 He, Z.H., Tian, F.Q., Gupta, H., Hu, H.C., Hu, H.P.: Diagnostic calibration of a hydrological model in a mountain area by
674   hydrograph partitioning, Hydrol Earth Syst. Sci., 19, 1807–1826, 2015.

Herman, J.D., Kollat, J.B., Reed, P.M. and Wagener, T.: Technical Note: Method of Morris effectively reduces the computational demands of global sensitivity analysis for distributed watershed models, Hydrol. Earth Syst. Sci., 17, 2893–2903, doi: 10.5194/hess-17-2893-2013, 2013.

Hou, Z., Huang, M., Leung, L. R., Lin, G., and Ricciuto, D. M.: Sensitivity of surface flux simulations to hydrologic parameters based on an uncertainty quantification framework applied to the Community Land Model, J. Geophys. Res., 117, D15108, doi: 10.1029/2012JD017521, 2012.

Houle, E.S. Livneh, B. and Kasprzyk, J.R.: Exploring snow model parameter sensitivity using Sobol' variance decomposition, Environmental Modelling & Software, 89, 144-158, 2017.

Hornberger, G., and Spear, R.: An approach to the preliminary analysis of environmental systems, J. Environ. Manage., 12, 7– 18, 1981.

Isenstein, E.M., Wi, S. Yang, Y.C. and Brown, C.: Calibration of a Distributed Hydrologic Model Using Streamflow and Remote Sensing Snow Data, World Environmental and Water Resources Congress 2015, 2015.

Islam, SU, Déry, S and Werner, AT.: Future Climate change Impacts on Snow and Water Resources of the Fraser River Basin, British Columbia, Journal of Hydrometeorology, doi: 10.1175/JHM-D-16-0012.1, 2017.

Ismail, M.F., Naz, B.S., Wortmann, M. et al.: Comparison of two model calibration approaches and their influence on future projections under climate change in the Upper Indus Basin, Climatic Change, 163, 1227–1246, doi: https://doi.org/10.1007/s10584-020-02902-3, 2020.

Jackson, R. B., J. Canadell, J. R. Ehleringer, H. A. Mooney, O. E. Sala, and Schulze, E. D. : A global analysis of root distributions for terrestrial biomes, Oecologia, 108, 389–411, doi:10.1007/BF00333714, 1996.

Jafarzadegan, K. Merwade, V. and Moradkhani, H.: Combining clustering and classification for the regionalization of environmental model parameters: Application to floodplain mapping in data-scarce regions, Environmental Modelling and Software, 125, doi: https://doi.org/10.1016/j.envsoft.2019.104613, 2020.

Jiskoot, H. and Mueller, M.S.: Glacier fragmentation effects on surface energy balance and runoff: field measurements and distributed modelling, Hydrol. Process., 26, 1861–1875, 2012.

Jost, F., Moore, RD, Menounos, B and Wheate, R.: Quantifying the contribution of glacier runoff to streamflow in the upper Columbia River Basin, Canada, Hydrol. Earth Syst. Sci., 16, 849–860, 2012.

Kanishka, G. and Eldho, T.I.: Streamflow estimation in ungauged basins using watershed classification and regionalization techniques, J. Earth Syst. Sci, 129,186, doi: https://doi.org/10.1007/s12040-020-01451-8, 2020.

Kienzle, S. W.: A new temperature based method to separate rain and snow, Hydrol. Process., 22, 5067–5085, doi: https://doi.org/10.1002/hyp.7131, 2008.

Kuhn, M., 2003. Redistribution of snow and glacier mass balance from a hydrometeorological model, Journal of Hydrology, 282, 95–103, doi: https://doi.org/10.1016/S0022-1694(03)00256-7.

Lafleur, P.: Leaf conductance of four species growing in a subarctic marsh, Can. J. Bot., 66, 1367– 1375, doi: 10.1139/b88-192, 1988.

709 Larabi, S., St-Hilaire, A., Chebana, F. and Latraverse, M.: Multi-Criteria Process-Based Calibration Using Functional Data
710 Analysis to Improve Hydrological Model Realism, Water Resour Manage., 32, 195–211, doi: 10.1007/s11269-017-1803-6,
711 2018.

712 Levia, D.F., Nanko, K., Amasaki, H. et al.: Throughfall partitioning by trees, Hydrol. Process., 33, 1698-1708, 2019.

713 Liang, X., Lettenmaier, D. P., Wood, E. F., and Burges S. J.: A simple hydrologically based model of land-surface water and
714 energy fluxes for general-circulation models, J. Geophys. Res. Atmospheres, 99, 14415–14428, doi: 10.1029/94JD00483,
715 1994.

716 Lilhare, R. Pokorny, S. Déry, S.J., Stadynk, T.A. and Koenig, K. A.: Sensitivity analysis and uncertainty assessment in water
717 budgets simulated by the variable infiltration capacity model for Canadian subarctic watersheds, Hydrological Processes,
718 34, 2057–2075, doi: 10.1002/hyp.13711, 2020.

719 Liang, X., Wood, E. F., and Lettenmaier D. P.: Surface soil moisture parameterization of the VIC-2L model: Evaluation and
720 modification, Glob. Planet. Change, 13, 195–206, doi: 10.1016/0921- 8181(95)00046-1, 1996.

721 Lohmann, D., Raschke, E., Nijssen, B. and Lettenmaier, D.P.: Regional scale hydrology: II. Application of the VIC-2L model
722 to the Weser River, Germany, Hydrological Sciences Journal, 43:1, 143-158, doi: 10.1080/02626669809492108, 1998.

723 Mai, J. (2023). Ten strategies towards successful calibration of environmental models. Journal of Hydrology, 620(A),
724 129414. http://doi.org/https://doi.org/10.1016/j.jhydrol.2023.129414
725

726 Mai, J. and Cuntz M.: Computationally inexpensive identification of noninformative model parameters by sequential
727 screening: Efficient Elementary Effects (EEE) (v1.0), Zenodo https://doi.org/10.5281/zenodo.3620895., 2020.

728 Mai, J., Craig, J. R., and Tolson, B. A.: Simultaneously determining global sensitivities of model parameters and model
729 structure, Hydrology and Earth System Sciences, 24(12), 5835–5858, doi: http://doi.org/10.5194/hess-24-5835-2020,
730 2020.

731 Mai, J., Arsenault, R., Tolson, B. A., Latraverse, M., and Demeester, K.: Application of parameter screening to derive optimal
732 initial state adjustments for streamflow forecasting, Water Resources Research, 56(9), e2020WR027960, 2020.

733 Mai, J., Craig, J. R., Tolson, B. A., and Arsenault, R.: The sensitivity of simulated streamflow to individual hydrologic
734 processes across North America, Nature Communications, 13(1), 455, doi: http://doi.org/10.1038/s41467-022-28010-7,
735 2022.

736 Marshall, S.J., White, E.C., Demuthm M.D et al.: Glacier Water Resources on the Eastern Slopes of the Canadian Rocky
737 Mountains, Canadian Water Resources Journal, 36:2, 109-134, doi: 10.4296/cwrj3602823, 2011.

738 Matheussenm, B., Kisrschbaum, R.L., Goodman, I.A., O'Donnell, G.M., and Lettenmaier, D.P.: Effects of land cover change
739 on streamflow in the interior Columbia River Basin (USA and Canada), Hydrol. Process, 14, 867-885, 2000.

740 Melsen, L., Teuling, A., Torfs, P. Zappa, M. et al.: Representation of spatial and temporal variability in large-domain
741 hydrological models: case study for a mesoscale pre-Alpine basin, Hydrol. Earth Syst. Sci., 20, 2207–2226, doi:
742 10.5194/hess-20-2207-2016, 2016.

743 Mendoza, P. A., Clark, M. P., Barlage, M., Rajagopalan, B., Samaniego, L., Abramowitz, G., and Gupta, H.: Are we
744   unnecessarily constraining the agility of complex process-based models?, Water Resour. Res., 51 (1), 716– 728, doi:
745   http://doi.org/10.1002/2014WR015820, 2015.

746 Morris, M.D.: Factorial sampling plans for preliminary computational experiments, Technometrics, 33 (2), 161e174, doi:
747   http://dx.doi.org/10.2307/1269043, 1991.

748 Minder, J. R., Mote, P. W., and Lundquist, J. D.: Surface temperature lapse rates over complex terrain: Lessons from the
749   Cascade Mountains, J. Geophys. Res., 115, D14122, doi: 10.1029/2009JD013493, 2010.

750 Mizukami, N., Clark, M.P., Newman, A.J. Wood, A.W, Gutmann, E.D, Nijssen, B., Rakovec, O. and Samaniego, L.: Towards
751   seamless large-domain parameter estimation for hydrologic models, Water Resour. Res. 53, 8020-8040, doi:
752   10.1002/2017WR020401, 2017.

753 Munro, D. S.: Stomatal conductances and surface conductance modelling in a mixed wetland forest, Agric. For. Meteorol., 48,
754   235–249, doi: 10.1016/0168-1923(89)90071-3, 1989.

755 Nasanova, O.N., Gusev, M.Y. and Kovalev, Y.: Investigating the Ability of a Land Surface Model to Simulate Streamflow
756   with the Accuracy of Hydrological Models: A Case Study Using MOPEX Materials, Journal of Hydrometeorology, 10,
757   1128-1150, doi: 10.1175/2009JHM1083.1, 2009.

758 Nijssen, B., O'Donnell, G.M., Lettenmaier, D.P., Lohmann, D., Wood, E.F.: Predicting the discharge of global rivers, J. Clim.
759   14 (15), 3307e3323, 2001.

760 Oudin, L., Andréassian, V., Perrin, C., Michel, C. and Le Moine, N.: Spatial proximity, physical similarity, regression and
761   ungaged catchments: A comparison of regionalization approaches based on 913 French catchments, Water Resources
762   Research, 44, W03413, doi: 10.1029/2007WR006240, 2008.

763 Oubeidillah, A.A., Kao, S.C., Ashfaq, M., Naz, B.S. and Tootle, G.: A large-scale, high-resolution hydrological model
764   parameter data set for climate change impact assessment for the conterminous US, Hydrol. Earth Syst. Sci., 18, 67–84, doi:
765   10.5194/hess-18-67-2014, 2014.

766 Payne, J.T., Wood A.W., Hamlet, A.F., Palmer, R.N., and Lettenmaier, D.P.: Mitigating the effects of climate change on the
767   water resources of the Columbia River basin, Climatic Change, 62: 233–256, 2004.

768 Pelletier, J.D., Broxton, P.D., Hazenberg, P., Zeng, X., Troch, P.A., Niu, G., Williams, Z.C., Brunke, M.A., and Gochis, D.:
769   Global 1-km Gridded Thickness of Soil, Regolith, and Sedimentary Deposit Layers. ORNL DAAC, Oak Ridge, Tennessee,
770   USA, doi: https://doi.org/10.3334/ORNLDAAC/1304, 2016.

771 Pelto, B.M., Maussion, F., Menounos, B., Radić, V., and Zeuner, M.: Bias corrected estimates of glacier thickness in the
772   Columbia River Basin, Canada, Journal of Glaciology, 66(260), 1051–1063, doi: https://doi.org/ 10.1017/jog.2020.75,
773   2020.

774 Pianosi, F., Beven, K., Freer, J., Hall, J.W., Rougier, J., Stephenson, D.B., and Wagener, T.: Sensitivity analysis of
775   environmental models: A systematic review with practical workflow, Environmental Modelling & Software, 79, 214-232,
776   2016.

Razavi, T. and Coulibaly, P.: Streamflow Prediction in Ungauged Basins: Review of Regionalization Methods, J. Hydrol. Eng., 18, 8, 958-975, doi: 10.1061/(ASCE) HE.1943-5584.0000690, 2013.

Rakovec, O., Kumar, R., Attinger, S. and Samaniego, L.: Improving the realism of hydrologic model functioning through multivariate parameter estimation, Water Resour Res, 52, 7779–7792, doi: https://doi.org/10.1002/2016 WR019430, 2016.

Rakovec, O., Mizukami, N., Kumar, R., Newman, A., Thober, S., Wood, A. W., et al.: Diagnostic evaluation of large-domain hydrologic models calibrated across the contiguous United States, Journal of Geophysical Research: Atmospheres, 124, 13,991–14,007, doi: https://doi.org/1029/2019JD030767, 2019.

Rosero, E., Yang, Z.L., Wagener, T., Gulden, L. E., Yatheendradas, S., and Niu, G.Y.: Quantifying parameter sensitivity, interaction, and transferability in hydrologically enhanced versions of the Noah land surface model over transition zones during the warm season, J. Geophys. Res., 115, D03106, doi:10.1029/2009JD012035, 2010.

Roux, M.: A Comparative Study of Divisive and Agglomerative Hierarchical Clustering Algorithms, Journal of Classification, 35, 345-366, doi: 10.1007/s00357-018-9259-9, 2018.

Samaniego, L., Kumar, R., and Attinger, S.: Multiscale parameter regionalization of a grid-based hydrologic model at the mesoscale, Water Resour. Res., 46, W05523, doi:10.1029/2008WR007327, 2010.

Samuel, J., Coulibaly, P., and Metcalfe, R.: Estimation of continuous streamflow in Ontario ungauged basins: Comparison of regionalization methods, J. Hydrol. Eng., 16(5), 447–459, 2011.

Saltelli, A.: Making best use of model valuations to compute sensitivity indices, Comput. Phys. Commun., 145 (2), 280e297, doi: http://dx.doi.org/10.1016/S0010-4655(02)00280-1, 2002.

Saltelli, A., Ratto, M., Andres, T., Campolongo, F., Cariboni, J., Catelli, D., Saisana, M., Tarantola, S.: Global Sensitivity Analysis, The Primer Wiley, 2008.

Sarrazin, F. Pianosi, F. and Wagener, T.: Global Sensitivity Analysis of environmental models: Convergence and validation, Environmental Modelling & Software, 79, 135-152, 2016.

Sawicz, K., Wagener, T., Sivapalan, M., Troch, P.A. and Carrillo, G.: Catchment classification: empirical analysis of hydrologic similarity based on catchment function in the eastern USA, Hydrol. Earth Syst. Sci. Discuss., 8, 4495–4534, doi: 10.5194/hessd-8-4495-2011, 2011.

Schnorbus, M. A.: VIC-Glacier (VIC-GL): Description of VIC Model Changes and Upgrades, VIC Generation 2 Deployment Report, Volume 1, Pacific Climate Impacts Consortium, University of Victoria, Victoria, BC, 40 pp, 2018.

Shafii, M. and Tolson, B. A.: Optimizing hydrological consistency by incorporating hydrological signatures into model calibration objectives, Water Resour. Res., doi: 10.1002/2014 WR016520, 2015.

Shafii, M., Basu, N., Craig, J.R., Schiff, S.L., and Van Cappellen, P.: A diagnostic approach to constraining flow partitioning in hydrologic models using a multiobjective optimization framework, Water Resour Res., doi: https://doi.org/10.1002/2016WR019736, 2017.

Schenk, H. J., and Jackson, R. B.: The global biogeography of roots, Ecol. Monogr., 72, 311–328, doi: 10.1890/0012-9615(2002)072[0311:TGBOR]2.0.CO2, 2002.

811 Schnorbus, M. A., Bennett, K.E., Werner, A.T., and Berland, A.J.: Hydrologic Impacts of Climate Change in the Peace,
812   Campbell and Columbia Watersheds, British Columbia, Canada, Pacific Climate Impacts Consortium, University of
813   Victoria: Victoria, BC, 2011.

814 Schnorbus, M. A., Werner, A., and Bennett, K.: Impacts of climate change in three hydrologic regimes in British Columbia,
815   Canada, Hydrol. Process., 28, 1170–1189, doi: https://doi.org/10.1002/hyp.9661, 2014.

816 Sellers, P. J.: Canopy reflectance, photosynthesis and transpiration, Int. J. Remote Sens., 6, 1335– 1372, doi:
817   10.1080/01431168508948283, 1985.

818 Sepúlveda, U.M., Mendoza, P.A., Mizukami, N. and Newman, A.J.: Revisiting parameter sensitivities in the Variable
819   Infiltration Capacity model, Hydrology and Earth System Sciences Discussions, doi: https://doi.org/10.5194/hess-2021-
820   550, 2021.

821 Sheikholeslami, R., Razavi, S., Gupta, H.V., Becker, W. and Haghnegahdar, A.: Global sensitivity analysis for high-
822   dimensional problems: How to objectively group factors and measure robustness and convergence while reducing
823   computational cost, Environmental Modelling & Software 111, 282-299, 2019.

824 Shrestha, R.R., Schnorbus, M. A., Werner, A.T. and Berland. A.J.: Modelling spatial and temporal variability of hydrologic
825   impacts of climate change in the Fraser River basin, British Columbia, Canada, Hydrol. Process., 26, 1840–1860, 2012.

826 Shrestha, R. R., Cannon, A. J., Schnorbus, M. A., and Zwiers, F. W.: Projecting future nonstationary extreme streamflow for
827   the Fraser River, Canada, Climatic Change, 145, 289–303, doi: https://doi.org/10.1007/s10584-017-2098-6, 2017.

828 Shrestha, R. R., Cannon, A. J., Schnorbus, M. A., and Alford, H.: Climatic Controls on Future Hydrologic Changes in a
829   Subarctic River Basin in Canada, J. Hydrometeor., 20, 1757–1778, doi: https://doi.org/10.1175/JHM-D-18-0262.1, 2019.

830 Schulze, E.-D., Kelliher, F. M., Korner, C., Lloyd, J., and Leuning, R.: Relationships among maximum stomatal conductance,
831   ecosystem surface conductance, carbon assimilation rate, and plant nitrogen nutrition: A global ecology scaling exercise,
832   Annu. Rev. Ecol. Syst., 25, 629–660, 1994.

833 Shin, M-J, Guillaume, J.H.A., Croke, B.F.W., and Jakeman, A. J.: Addressing ten questions about conceptual rainfall–runoff
834   models with global sensitivity analyses in R. Journal of Hydrology 503,135–152, 2013.

835 Simard, M., Pinto, N., Fisher, J. B., and Baccini, A.: Mapping forest canopy height globally with spaceborne lidar, J. Geophys.
836   Res. Biogeosciences, 116, G04021, doi: 10.1029/2011JG001708, 2011.

837 Sobol', I.M.: Sensitivity estimates for nonlinear mathematical models, Matematicheskoe Modelirovanie 2, 112-118 (in
838   Russian), translated in English (1993), In: Mathematical Modelling and Computational Experiments, 1(4), pp. 407-414,
839   1990.

840 Toney, C., and Reeves, M. C.: Equations to convert compacted crown ratio to uncompacted crown ratio for trees in the Interior
841   West, Western Journal of Applied Forestry, 24(2), 76–82, 2009.

842 Troy, T.J., Wood, E.F. and Sheffield J.: An efficient calibration method for continental-scale land surface modelling, Water
843   Resour. Res. 44, W09411, doi: 10.1029/2007WR006513, 2008.

844 Van Griensven, A., Meixner, T., Grunwald, S., Bishop, T., Diluzio, M., and Srinivasan, R.: A global sensitivity analysis tool
845   for the parameters of multi-variable catchment models, Journal of Hydrology, 324(1), 10–23, 2006.

846 Vihma, T.: Atmosphere-Snow/Ice Interactions. Encyclopedia of Snow, Ice and Glaciers, V.P. Singh, P. Singh, and U.K.
847   Haritashya, Eds., Springer Netherlands, 66–75, 2011.

848 Waheed, S.Q., Grigg, N.S., Ramirez, J.A.: Variable Infiltration-Capacity Model Sensitivity, Parameter Uncertainty, and Data
849   Augmentation for the Diyala River Basin in Iraq, J. Hydrol. Eng., 25(9), doi: 10.1061/(ASCE)HE.1943-5584.0001975,
850   2020.

851 Wang, T.L., Hamann, A., Spittlehouse, D.L., Murdock, T.Q.: ClimateWNA--High-Resolution Spatial Climate Data for
852   Western North America, Journal of Applied Meteorology and Climatology, 51 (1), 16–29, doi: 10.1175/JAMC-D-11-
853   043.1, 2012

854 Wallner, M., Haberlandt, U., and Dietrich, J.: A one-step similarity approach for the regionalization of hydrological model
855   parameters based on self-organizing maps, J. Hydrol., 494, 59–71, doi: 10.1016/j.jhydrol.2013.04.022, 2013.

856 Wenger, S. J., Luce, C. H., Hamlet, A. F., Isaak, D. J., and Neville, H. M.: Macroscale hydrologic modeling of ecologically
857   relevant flow metrics, Water Resour. Res., 46, W09513, doi: 10.1029/2009WR008839, 2010.

858 Werner, A. T., Schnorbus, M. A., Shrestha, R. R., Cannon, A. J., Zwiers, F. W., Dayon, G. and Anslow, F.: A long-term,
859   temporally consistent, gridded daily meteorological dataset for northwestern North America, Sci. Data, 6, 180299, 2019.

860 Woods, R.A.: Analytical model of seasonal climate impacts on snow hydrology: Continuous snowpacks, Advances in Water
861   Resources, 32, 1465-1481, doi: 10.1016/j.advwatres.2009.06.011, 2011.

862 Xie Z. and Yuan, F.: A parameter estimation scheme of the land surface model VIC using the MOPEX databases, Large
863   Sample Basin Experiments for Hydrological Model Parameterization: Results of the Model Parameter Experiment–
864   MOPEX. IAHS Publ. 307, 2006.

865 Xue, X., Zhang, K., Hong, Y. et al.: New Multisite Cascading Calibration Approach for Hydrological Models: Case Study in
866   the Red River Basin Using the VIC Model, J. Hydrol. Eng., 2016, 21(2): doi: 10.1061/(ASCE)HE.1943-5584.0001282.,
867   2015.

868 Yadav, M., Wagener, T., Gupta, H.: Regionalization of constraints on expected watershed response behavior for improved
869   predictions in ungauged basins. Advances in Water Resources, 30, 1756–1774, 2007.

870 Yanto, Livneh, B. Rajagopalan, B. and Kasprzyk, J.: Hydrological model application under data scarcity for multiple
871   watersheds, Java Island, Indonesia, Journal of Hydrology: Regional Studies, 9, 127–139, doi:
872   https://doi.org/10.1016/j.ejrh.2016.09.007, 2017.

873 Yilmaz, K. K., Gupta, H. V. and Wagener, T.: A process-based diagnostic approach to model evaluation: Application to the
874   NWS distributed hydrologic model, Water Resour. Res., W09417, doi: 10.1029/2007WR006716, 2008.

875 Young, P.C., Spear, R.C., Hornberger, G.M.: Modelling badly defined systems: some further thoughts. In: Proceedings
876   SIMSIG Conference, Canberra, pp. 24-32, 1978.

877